https://doi.org/10.5194/egusphere-2025-4712
Preprint. Discussion started: 12 November 2025


# The Oxygen Minimum Zones (OMZs) in the Indian Ocean

**Eugene Oboh[1,3], Niko Lahajnar[2], Birgit Gaye[2], Avanti Shrikumar[4], Tim Rixen[1]**
[1]Leibniz Centre for Tropical Marine Research (ZMT), Bremen, 28359, Germany,
[2]University of Hamburg, Institute for Geology, Hamburg, 20146, Germany,
[3]University of Bremen, Bremen, 28359, Germany,
[4]University of Sydney, Charles Perkins Center, NSW 2006, Australia.

*Correspondence to*: Eugene Oboh (oboh.eugene@leibniz-zmt.de)

**Abstract.** The Oxygen Minimum Zones (OMZs) in the northern Indian Ocean (i.e., the Arabian Sea and the Bay of Bengal) are among the most intense OMZs in the world's oceans. While there is no clear evidence of a significant change in the Bay of Bengal (BoB) OMZ, the Arabian Sea (AS) OMZ followed the global trend and expanded in the last decades until 2013. Since then, however, this trend has reversed, and the AS OMZ seems to have shrunk. The stability of the BoB OMZ as well as the expansion and shrinkage of the AS OMZ in response to global warming is poorly understood. In this study we redefined the water masses and employed an extended Optimum Multiparameter (eOMP) Analysis to investigate changes in the oxygen supply due to mixing and biological oxygen consumption dynamics in these OMZs based on empirical field data from the Global Ocean Data Analysis Project version 2 (GLODAPv2) and a research cruise conducted with a German research vessel Sonne in 2024. Our findings reveal in line with previous studies a reversal in the expansion trend of the AS OMZ but also a shrinkage of the BoB OMZ between 1995 and 2016. In both regions this is due to an increased northward influx of oxygen-rich water masses from southern Indian Ocean, combined with a reduced contribution from relatively oxygen-poor local and equatorial water masses. However, we also observed that increased physical oxygen supply was accompanied by an increased biological oxygen consumption. These changes are likely linked to the slowdown of the global thermohaline circulation in the Indian Ocean. The slowdown is accompanied by a reduced inflow of the Indonesian Throughflow Water into the Indian Ocean and a lower output of Indian Ocean waters via the Agulhas Current/Leakage (at 32°S) into the Atlantic Ocean. A resulting increase in the residence time of water masses in the Indian Ocean is consistent with the detected biological oxygen consumption while the weaker zonal circulation seems have favored the meridional circulation which carried water from the southern Indian Ocean northwards. This implies a coupling between the OMZ in the Indian Ocean and climate change via the effect of the latter on the global thermohaline circulation as also seen in palaeoceanographic archives, whereas the drivers in past and today differs.

https://doi.org/10.5194/egusphere-2025-4712
Preprint. Discussion started: 12 November 2025


## 1 Introduction

The decline of dissolved oxygen in the ocean is one of the greatest threats to the ocean (Breitburg et al., 2018). It affects biogeochemical cycles, endangers marine ecosystems, and ultimately jeopardizes our food security because almost all economically relevant marine organisms are animals and need oxygen to breathe (Stramma et al., 2008; Stramma et al., 2010). The decrease in dissolved oxygen is primarily attributed to global warming and the associated warming of ocean water because the latter reduces the solubility of oxygen in water (Benson & Krause Jr., 1980). Global warming does not only affect the surface of the ocean but also the oxygen minimum zones (OMZs) in the interior of the ocean (Stramma et al., 2008). OMZs result from the interplay between the physical oxygen supply and the biological oxygen consumption and develop mainly below the surface mixed layer in water depths of about 100–600 m (Sverdrup, 1938). The production of organic matter by phytoplankton, its subsequent export and respiration by bacteria and zooplankton below the photic zone controls the oxygen consumption (Sigman & Hain, 2012; Malone et al., 2015). The intrusion of former well-oxygenated surface water masses into an oxygen minimum zone (OMZ) is in turn the main oxygen supply mechanism. In addition to vertical mixing and associated variations of the surface mixed layer depth (MLD), oxygen is supplied by isopycnical mixing (Duteil & Oschlies, 2011; Rudnickas et al., 2019). Water masses that ventilate these OMZs are formed at high latitudes in association with the deep and mode water formation (Broecker, 1991; Sarmiento et al., 2004) as well as in regions where evaporation or cooling increases the density of the surface water until it becomes denser than the water below and begins to sink. In addition to the supply of oxygen, the residence time of water in the OMZs influences the oxygen concentration within them (Rixen & Ittekkot, 2005; Rixen et al., 2020). Hence, ventilation decreases when the incoming water mass has a lower oxygen concentration and remains in the OMZ for a longer period as this increases OMZ exposure to the biological oxygen consumption.

Although OMZs can be observed almost everywhere in the ocean, they are most intense in the eastern tropical Pacific, the Arabian Sea, and the Bay of Bengal. The latter two are the semi-enclosed basins in the northern Indian Ocean, where oxygen levels drop below 20 µmol kg$^{-1}$. At such low oxygen concentrations, oxygen loses its inhibitory function and anoxic begin to outcompete oxic microbial processes. This oxic/anoxic transition is termed microbial hypoxia and represents the lower range of hypoxia (Rixen et al., 2020). Hypoxia defines the oxygen threshold below which higher organism respond to the lack of oxygen and it already sets in if oxygen concentration falls below approximately 120–63 µmol kg$^{-1}$ (Ekau et al., 2010).

Climate projections under all Share Socioeconomic Pathways predict a decrease in the globally averaged OMZ oxygen concentration (i.e. water depth between 100–600 m), while projections at the regional level show considerable variations (Kwiatkowski et al., 2020). Nevertheless, the largest decreases in oxygen concentrations are expected to occur at higher latitudes, while rising oxygen concentrations are projected for equatorial regions. In the Indian Ocean the increasing equatorial oxygen concentrations have been associated with decreasing oxygen consumption (Kwiatkowski et al., 2020) and an enhanced inflow of oxygen-enriched water masses from the Southern Ocean (Ditkovsky et al., 2023). However, the northern Arabian Sea appears to be an exception with predictions indicating that the OMZ will intensify in the future (Kwiatkowski et al., 2020; Ditkovsky et al., 2023). Since the Arabian Sea OMZ (AS OMZ) is already at the transition towards anoxia, even minor changes could have significant effects (Rixen

https://doi.org/10.5194/egusphere-2025-4712
Preprint. Discussion started: 12 November 2025


et al., 2020). However, the OMZ in the northern Indian Ocean are poorly represented in climate models (Rixen et al., 2020; Parvathi Vallivattathillam et al., 2023) due to uncertainties of almost all processes affecting the OMZs ventilation (Schmidt et al., 2021).

Nevertheless, in line with model results, data collected prior to 2007 reveal an expansion of the AS OMZ (Banse et al., 2014; Rixen et al., 2014; Goes et al., 2020) due to both an increased oxygen consumption and a reduced ventilation. The first was assumed to be a consequence of enhanced biological productivity in surface water (Lachkar et al., 2018) and the second was related to the warming and thus a lower inflow of Persian Gulf Water (PGW) into the AS OMZ (Lachkar et al., 2019). In contrast to this observed and projected trend, a recent Argo float study showed that the AS OMZ has been shrinking since 2013 due to a decline in surface ocean productivity (Liu et al., 2024). Furthermore, Liu et al. (2024) noted an upward trend in dissolved oxygen in the AS OMZ between 2013 and 2022, except for a brief decline from 2016 to 2018. This decline coincided with the negative Indian Ocean Dipole (IOD) event in 2016 and the weak La Niña event in 2017-2018. Such combination of climate anomalies could enhanced summer monsoon winds and upwelling off Oman (Thushara et al., 2019; Qadimi et al., 2021), thereby boosting productivity and subsequently oxygen consumption at intermediate depths. On longer time-scales, paleoceanographic archives show close link between the intensity of the Arabian Sea OMZ to the Greenland ice core record (Schulz et al., 1998; Altabet et al., 1999; Suthhof et al., 2001). This indicates strong links between north Atlantic climate anomalies and the Arabian Sea OMZ but the mechanisms are not yet clear.

The Bay of Bengal OMZ (BoB OMZ) in turn is less intense than that in the Arabian Sea and has remained relatively stable (Johnson et al., 2019; Nayak et al., 2024). Analyses by Sridevi and Sarma (2020) in line with that from Bhaskar et al. (2021) revealed that a balance among physical forcings including salinity stratification, occurrence of cyclonic and anticyclonic eddies was responsible for this oxygen stability.

In order to better understand the resilience of the BoB OMZ to global warming as well as the trend reversal of the AS OMZ, we performed an Extended Optimum Multiparameter (eOMP) analysis (Tomczak & Large, 1989), based on empirical field data from the Global Ocean Data Analysis Project version 2 (GLODAPv2). This data-based analysis indicates the composition of the water masses in the OMZs and the associated physical oxygen supply via the inflow of individual water masses. It also shows the biological oxygen consumption as the difference between the physical oxygen supply and the measured oxygen concentration.

https://doi.org/10.5194/egusphere-2025-4712
Preprint. Discussion started: 12 November 2025


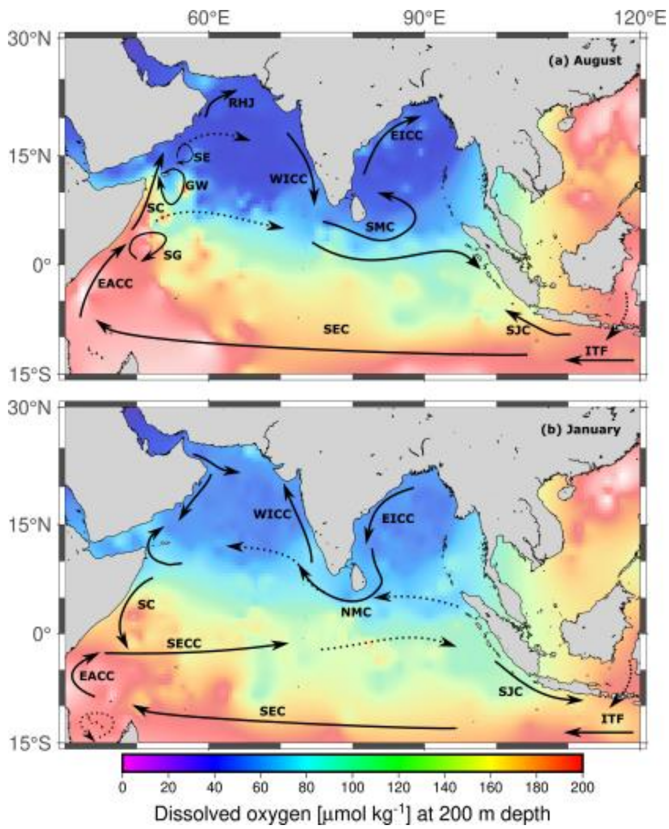


**Figure 1: Surface currents in the Indian Ocean during (a) the summer monsoon in August and (b) the winter monsoon in January. Abbreviations: Somali current (SC), South Equatorial Current (SEC), East African Coastal Current (EACC), Southern Gyre (SG), Socotra Eddy (SE), Great Whirl (GW), Southwest Monsoon Current (SMC), East Indian Coastal Current (EICC), Northeast Monsoon Current (NMC), West Indian Coastal Current (WICC), Indonesian throughflow (ITF), Ras al Hadd jet (RHJ), South Java Current (SJC).**

### 1.1 Study Area

The Indian Ocean differs from other ocean basins mainly due to its geographical characteristics, which have far-reaching consequences for atmospheric and oceanic circulation. The first unique geographical feature is the Asian landmass. This landmass limits the northern extent of the Indian Ocean in the subtropics at about 30° N, leading to the development of the Asian monsoon. The monsoon is well-known for its seasonally changing wind direction and heavy rainfall. This rainfall makes the dry Indian countryside to blossom in summer and also causes rivers to swell, especially in Bangladesh where the Ganges Brahmaputra River system enters the ocean (i.e., Bay of Bengal). Heavy monsoon rains can cause severe flooding (Gadgil et al., 2007). The monsoon is driven by the intense summer heating of the Asian landmass and in particular the Tibetan plateau (Prell & Kutzbach, 1992). The resulting extreme atmospheric summer low over the Asian continent attracts the South East trade wind from the southern hemisphere which change direction and blow largely as South West (SW) winds over the northern Indian Ocean after crossing the equator. In contrast and similar to the other major ocean basins, the northern Indian Ocean is exposed to the North

https://doi.org/10.5194/egusphere-2025-4712
Preprint. Discussion started: 12 November 2025


East (NE) trade winds in winter. These seasonal changes of wind direction from NE to SW reverse the surface currents in the northern Indian Ocean (Fig. 1), leading to an overall clockwise surface circulation in summer and a counterclockwise circulation in the winter (Wyrtki, 1973; Phillips et al., 2021). In summer, Arabian Sea water flows along with the surface currents into the Bay of Bengal, while the reversal of the current system enables the inflow of Bay of Bengal water into the Arabian Sea in winter.

The second unique geographical feature of the Indian Ocean is the Indonesian Archipelago. It allows the inflow of waters form the Pacific into the Indian Ocean and represents the only connection between major ocean basins at low latitudes (Gordon et al., 2003; Gordon et al., 2010). Nevertheless, the circulation in the southern Indian Ocean is similar to that in other ocean basins. The subtropical gyre is located in the center of the basin and is framed by three major boundary currents. The South Equatorial Current (SEC) represents the northern part, while the South Indian Current (SIC) forms the southern part of the subtropical gyre. The Subantarctic Front separates the SIC from Southern Ocean and the Antarctic Circumpolar Current (Phillips et al., 2021). The Agulhas Current (AC) off Africa builds the western boundary of the subtropical gyre. It connects the SEC and SIC but it also creates a passageway through which Indian Ocean water escapes into the Atlantic Ocean. Both, the AC and the Indonesian Throughflow (ITF) act as bottlenecks within the surface water return flow of the global Thermohaline Ocean Circulation (Broecker, 1991; Durgadoo et al., 2017). The SEC and the AC connect these bottlenecks and carry Indonesian Throughflow Water (ITFW) through the Indian Ocean into the Atlantic Ocean. However, off Australia the ITFW also feeds the southwards flowing Leeuwin Current (LC) which hinders the development of an eastern boundary current similar to the Benguela and Humboldt Currents in the South Atlantic and Pacific Ocean, respectively. In the shadow of these currents emerge the well-known and high productive eastern boundary upwelling systems (Kämpf & Chapman, 2016; Hood et al., 2017). In the Indian Ocean such eastern boundary upwelling systems are absent, but pronounced monsoon-driven (i.e. seasonal) upwelling systems occur south off Java, around the southern tip of India in the Arabian Sea and off Sri Lanka as well as off Somalia and the Arabian Peninsula (Rixen et al., 1996; Rixen et al., 2006; Wiggert et al., 2006).
Upwelling systems influence the OMZ because they favor the production of organic matter in the photic zone of the ocean, thereby affecting biological oxygen consumption. As part of the Indian Ocean Meridional Overturning Circulation (MOC), they also influence the ventilation of the OMZ. In particular the strong upwelling systems off Somalia and in the Arabian Sea play a significant role in the MOC of the Indian Ocean. The Indian Ocean MOC consists of a shallow and deep overturning cell, with the shallow cell encompassing the upper 300 – 450 m and the deep cell water masses below this depth-range (Schott & McCreary Jr, 2001; Stramma et al., 2002).
The shallow MOC links upwelling to the formation of subsurface water masses. The latter occurs in the vicinity of the Subantarctic Front and, to a lesser extent, at the outflow of Red Sea Water (RSW) and Persian Gulf Water (PGW) as well as in the central Arabian Sea. North of the Subantarctic Front in the southern part of the subtropical gyre as well as in the other three regions, evaporation exceeds freshwater fluxes (i.e., precipitation and river run-off) with the result that salty and dense water forms and sinks. The high salinity Subtropical Surface Water (STSW) forms preferentially between 25°S and 35°S and at around 90°E (Wyrtki et al., 1971; Beal et al., 2006) whereas the Arabian Sea High Salinity Water (ASHSW) forms preferentially in spring, when the Arabian Sea begins to warm up and the depth of the

https://doi.org/10.5194/egusphere-2025-4712
Preprint. Discussion started: 12 November 2025


winter mixed layer (MLD) flattens out. The RSW and the PGW, which enter the Arabian Sea, can be found at depths of around 300–1000 m and 250–300 m, respectively (Tchernia, 1980; Beal et al., 2000; Bower et al., 2000).
South of the Subantarctic Front at around 50°S–40°S, low salinity but cool and thus dense water is subducted below the warmer and lighter subtropical water masses from north of the Subantarctic Front (Talley, 1996; Saenko & Weaver, 2001). The Antarctic Intermediate Water (AAIW) is the deepest of these mode waters and circulates with the Antarctic Bottom Water (AABW) in the deep MOC. The AABW forms around the Antarctic continental margins and four main formation regions have been identified, two of which are located in the Indian Ocean sector of Southern Ocean: the Cape Darnley polynya (65°E–69°E) and the Enderby Basin (136°E–154E) (Menezes et al., 2017). Since the AABW undergoes significant modification due to mixing in the abyssal Indian Ocean (Mantyla & Reid, 1995), it is referred to as Modified Antarctic Bottom Water (mAABW).
Due to the entrainment of nutrient-enriched subsurface water into the photic zone via upwelling in summer and mixed layer deepening in winter, the Arabian Sea belongs to the most productive regions of the ocean similar to eastern boundary upwelling systems in the other ocean basins (Wyrtki et al., 1971; Kumar et al., 2000). While productivity reveals pronounced seasonality, with higher rates of organic matter export in summer than in winter, the Arabian Sea oxygen minimum zone (AS OMZ) shows only weak seasonality, as upwelling and winter mixed layer deepening also favor OMZ ventilation (Sarma, 2002; Resplandy et al., 2012). In turn, the Bay of Bengal and the entire eastern equatorial Indian Ocean are strongly influenced by high freshwater fluxes as indicated by the low sea surface salinity (Vinogradova et al., 2019). This low salinity surface water forms a buoyant surface layer that reduces productivity by hindering the entrainment of nutrient-enriched subsurface waters into the euphotic zone (Rixen et al., 2006).
The Indian Ocean is also affected by events such as the Indian Ocean Dipole (IOD) and El Niño-Southern Oscillation (ENSO) cycles. The IOD is associated with enhanced rainfall in Indonesia and Australia as well as droughts in East Africa, while ENSO is responsible for irregular climate fluctuations in the tropical Ocean (Saji et al., 1999; Ashok et al., 2001; Wang & Picaut, 2004). ENSO consists of three phases; the El Niño phase (warm SST and weakened trade winds), the La Niña phase (cooler SST and stronger trade winds, intensified rainfall in southeast Asia) and the neutral phase. Negative IOD events and La Niña could strengthen summer monsoon winds, boosting upwelling off Oman in the Indian Ocean (Thushara et al., 2019; Qadimi et al., 2021).

## 2 Methods

We conducted an eOMP analysis to improve our understanding of the resilience of the BoB OMZ to global change as well as the trend reversal of the AS OMZ. This involved investigating changes in water mass composition, physical oxygen supply as well as changes in biological oxygen consumption, all of which are crucial for understanding the variations in dissolved oxygen levels within the OMZs.

https://doi.org/10.5194/egusphere-2025-4712
Preprint. Discussion started: 12 November 2025


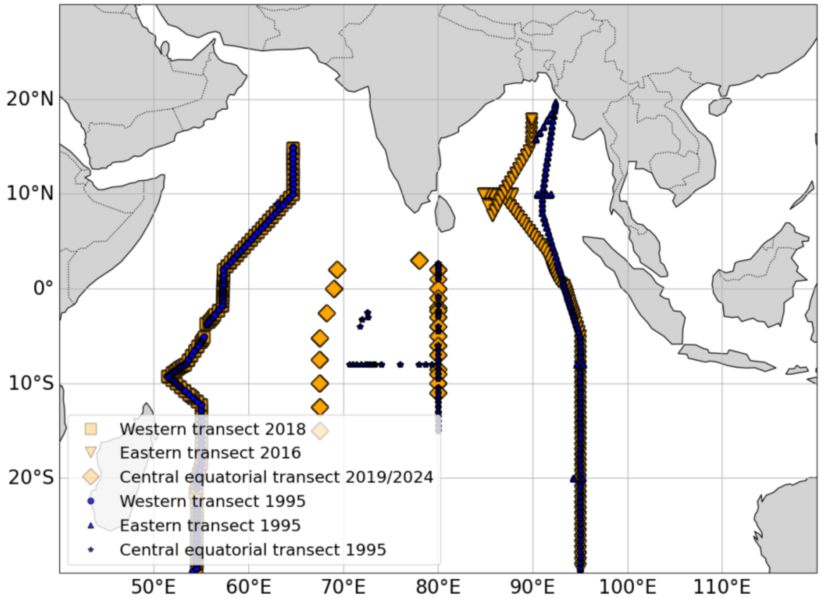


**Figure 2: Data transect showing 1995, 2016, 2018, 2019 data sets from GLODAPV2 data and a mix of 2019 GLODAPV2 data and 2024 sonne cruise data for the Central equatorial transect 2019/2024.**

## 2.1 Data collection

We obtained empirical field data from the GLODAPv2 dataset (Olsen et al., 2019; Lauvset et al., 2022). The data consists of transects from 1995 and 2018 in the western Indian Ocean and transects from 1995 and 2016 in the eastern Indian Ocean as well as transects from 1995 and 2019 at the central equatorial Indian Ocean (Fig. 2). We selected western and eastern transects because they extend into the northern Indian Ocean OMZs, therefore, are important in representing the OMZs which could extend up to 20°S with its core in the northern end of the transects. The GLODAPv2 dataset provides oceanographic data from the surface to a depth of 4000 m and includes key parameters such as temperature, salinity, dissolved oxygen, nitrate, and phosphate. We specifically used the merged data product from GLODAPv2, which has undergone extensive quality control, including systematic bias evaluations and corrections for calibration and measurement errors (Olsen et al., 2019). In addition to GLODAPv2, we incorporated field data collected during the SONNE SO303 cruise in February 2024 (Fig. 2), which took place near the equator in the central Indian Ocean. These data include the aforementioned parameters: temperature, salinity, dissolved oxygen, nitrate, and phosphate (Gaye et al., 2024).

The entire western and eastern transects were analyzed along a depth range between 150 and 1200 m. This filtering enables us to exclude the upper ocean surface waters with a high variability and focuses on intermediate depths, which aligns with the depth range of OMZs. Furthermore, we defined the core of the OMZs within the transects as regions where the dissolved oxygen concentration falls below 20 µmol kg$^{-1}$. This corresponded to depths between 150 and 1000 m for the AS OMZ, and 150 and 800 m for the BoB OMZ. We filtered the western and eastern transects along

https://doi.org/10.5194/egusphere-2025-4712
Preprint. Discussion started: 12 November 2025


latitudes between 15° S and 3° N to obtain equatorial transects for both regions. For the central equatorial region, we compared the 1995 GLODAPv2 data to a combination of the 2019 GLODAPv2 and the 2024 cruise data. The later data were combined to increase the size of data.

#### 2.1.1 Primary productivity and Sea Surface Temperature data

Ocean primary productivity data from (Kulk et al., 2020) was used to analyze productivity in the Arabian Sea. The data was accessed on March 26, 2025 and consists of monthly global marine phytoplankton primary production data at a 9 km resolution between 1998–2020. This data was filtered for the Arabian Sea between 5° N and 25° N and 50° E and 75° E, and the annual mean was plotted to observe the trend.
This data is available at https://catalogue.ceda.ac.uk/uuid/69b2c9c6c4714517ba10dab3515e4ee6/. Likewise, sea surface temperature (SST) data "NOAA OI SST V2 High Resolution Dataset" provided by NOAA on their website at https://psl.noaa.gov/data/gridded/data.noaa.oisst.v2.highres.html was accessed on July 20, 2025. It consists of weekly mean SST data from 1981 to 2025 at a resolution of 0.25°. We filtered this data for the Indian Ocean region (30° N–30° S, 30° E–120° E) and plotted the yearly mean SSTs and 5-years running mean SSTs to observe the trend across the Indian Ocean.

#### 2.1.2 World Ocean Atlas data

Data used for water mass definition was collected from the World Ocean Atlas (WOA) database. This data consists of annual temperature and salinity means from time periods 1995–2004 and 2015–2022, and all time periods data for oxygen, phosphate and nitrate. As the GLODAPv2 data lacks coverage in the key source regions where the relevant water masses form or enter into the Indian Ocean therefore, we used the WOA data for water mass definition.

### 2.2 Optimum multi-parameter (OMP) analysis

The OMP analysis is a mathematical technique developed by Tomczak and Large (1989) to study water mass mixing in a given region. In this approach, a water sample is considered to be a mixture of multiple water masses. The objective of the analysis is to determine the fraction of each water mass in the water sample. This is achieved by using a non-negative least square method to estimate the contribution of each water mass for a given measurement point of the sample. For this study the eOMP analysis was performed using a Python-based model called PYOMPA (Shrikumar et al., 2022). PYOMPA is based on the original OMP analysis by Tomczak and Large (1989). The mathematical formula used to solve the objective function is presented in Eq. (1):

$$\left(\sum_i e_p^i x_j^i\right) + r_B^A \Delta_j^B = s_p^j + \epsilon_p^j \qquad (1)$$

Here, $s_p^j$ denote the value of the property *p* in measured water sample *j*,
$x_j^i$ stands for the estimated fraction of water mass *i* in sample *j*,
$e_p^i$ stands for the value of property *p in the* water mass,

https://doi.org/10.5194/egusphere-2025-4712
Preprint. Discussion started: 12 November 2025


$\epsilon_p^j$ denotes the residual in explaining property *p* for sample *j*,

$r_B^A \Delta_j^B$ represents the biogeochemical terms, where $r_B^A$ denotes the exchange ratio of two properties *A* and *B,* while $\Delta_j^B$ denotes the amount of property *B* that is re-mineralized due to the consumption of property *A* in sample *j*.

To regulate the effect of any properties on the equation, weights are numerical values assigned to each property. The bigger the weight, the higher the solution is controlled by that property. The residual equation is presented in Eq. (2),

$$\epsilon_p^j = \frac{W_p^{user}}{\sigma_p}\left(\left(\sum_i (e_p^i - \mu_p)x_j^i\right) + r_B^A \Delta_j^B - \left(s_p^j - \mu_p\right)\right) \quad (2.)$$

where $\mu_p$ represent the property mean. In this study we adopted parameter weight approach of Acharya and Panigrahi (2016) in the Arabian Sea region (see Table 2). Remineralization was tracked as a conversion of oxygen to phosphate and nitrate according to the ratio -155:1:15, adopted from Hupe and Karstensen (2000). The low parameter residue in objective (<0.25%) and low mass residual (< 0.0028) recorded by the majority (>99.9%) of the water samples show that the water samples were well represented by the water masses included in our eOMP analysis (Poole & Tomczak, 1999; Shrikumar et al., 2022).

Additionally, we performed a sensitivity analysis to assess the sensitivity of the model solution to $O_2$:$PO_4$:$NO_3$ remineralization ratios as well as to the parameter weights. For the remineralization ratios, we performed sensitivity analysis based on three $O_2$:$PO_4$:$NO_3$ ratio scenarios, -138:1:16 (the standard Red field ratios), -155:1:15 (Hupe & Karstensen, 2000) and -170:1:16 (Anderson & Sarmiento, 1994). For each scenario, we computed the model's root mean square (RMS) error from its total weighted sum of squared residuals and also computed the mean fraction of water masses. The results revealed that the scenario with the lowest oxygen ratio (i.e., $O_2$: −138) led to the highest RMS errors (0.7) and a more varied distribution of water masses compared to the other two scenarios, while ratios with $O_2$: -170 and $O_2$: -155 both had RMS less than 0.1 (Appendix Fig. 8). Although the −170:15:1 remineralization ratio yielded the lowest RMS error, we selected −155:15:1 to align more closely with standard Redfield stoichiometry, thereby ensuring biogeochemical realism in the model results rather than overfitting to local variability in the data.

Additionally, we conducted sensitivity analysis to evaluate how variations in individual parameter weights adopted from Acharya and Panigrahi (2016) influence model solution. Each weight (e.g., for temperature, salinity, oxygen, phosphate, and nitrate) was independently varied by ± 3 units from its baseline value while all other weights remained fixed. All runs used constant remineralization ratios ($O_2$:$PO_4$:$NO_3$ = −155:1:15). For each scenario, we computed the model's RMS error and mean water mass fractions. The results show that the model was more sensitive to changes in $PO_4$ and $NO_3$ and relatively stable to changes in other parameters (Appendix Fig. 9).

The PYOMPA implementation of OMP analysis differs from the traditional OMP analysis in certain ways. In PYOMPA conservation of mass is implemented as a hard constraint, therefore it looks for solutions where mass conservation results in zero residual. Additionally, it has support for flexible Redfield ratios when modeling remineralization (Shrikumar et al., 2022). However, we did not use any of these features and therefore reverted to the original method of Tomczak and Large (1989).

### 2.2.1 Physical oxygen supply and biological oxygen consumption analysis

Physical oxygen supply analysis determines the amount of oxygen ($O_2$) in the sample (*j*) supplied via mixing with a specific water mass ($s^{j}_{iO_2}$). Therefore, the fraction of the water mass ($x^{i}_{j}$) in the measured sample, *j* was multiplied by the defined oxygen concentration of the water mass ($e^{i}_{O_2}$) according to Eq. (3).

$$s^{j}_{iO_2} = x^{i}_{j} \text{ x } e^{i}_{O_2} \tag{3}$$

For biological oxygen consumption in a given sample (*j*) due to remineralization ($s^{j}_{-O_2}$), we used the measured oxygen in the sample ($s^{j}_{O_2}$), the overall oxygen due to mixing of all water masses ($\sum s^{j}_{nO_2}$), and the oxygen residual ($\epsilon^{j}_{O_2}$) according to Eq. (4):

$$s^{j}_{-O_2} = s^{j}_{O_2} - \left(\sum s^{j}_{nO_2}\right) + \epsilon^{j}_{O_2} \tag{4}$$

Oxygen consumption in this study represents the net biological oxygen utilization and it is closely related to Apparent Oxygen Utilization (AOU) (see Eq. 4). The data used to conduct the eOMP were obtained from the GLODAP database (Olsen et al., 2019) and during a cruise with the German research vessel Meteor in the Indian Ocean in 2024, hereafter regarded as cruise data.

## 2.3 Water mass definition

It is important to define water mass properties when performing eOMP analysis, as the latter relies on precise water mass definition in order to quantify mixing proportions and biogeochemical processes. This involves modelling a water sample as a linear combination of different water masses (Tomczak & Large, 1989; Shrikumar et al., 2022). A water mass is an identifiable body of water with distinct physical and chemical properties (e.g., temperature, salinity, oxygen and nutrients) that originates from a specific formation region and/or has a specific mixing history (Tomczak, 1999). These properties act as conservative or non-conservative tracers, which makes it possible to track the water mass movement (Tomczak, 1999).

The definition of water masses in the Indian Ocean is challenging. Many studies are based on water mass mixtures rather than the original water masses formed from the ocean surface, which are more relevant for assessing climate-driven changes (Acharya & Panigrahi, 2016; Ditkovsky et al., 2023). Additionally, inconsistencies in the definition of water mass properties across different studies complicate classification further (see Table 1). To address these issues, this study focuses specifically on water masses originating from the ocean surface.

https://doi.org/10.5194/egusphere-2025-4712
Preprint. Discussion started: 12 November 2025


To define the unique hydrological characteristics of these water masses, we utilized the World Ocean Atlas (WOA) dataset. First, we used literature sources to define the latitude, longitude and depth ranges in which these water masses enter/or form in the Indian Ocean. Thereafter, we filtered the WOA data accordingly for each water mass and calculated the mean values for key parameters, including temperature, salinity, oxygen, phosphate and nitrate (see Table 2). The specific latitude, longitude and depth ranges used for each water mass are shown in Table 3.

Water mass definition also helps us to account for warming-driven changes. We explicitly integrated the observed temperature shifts in the water masses into the eOMP analysis by using the water mass definition from 1995–2004 WOA data for 1995 eOMP analysis, and 2015–2022 WOA data sets for 2016, 2018, 2019 and 2024 analysis. This approach enables us to capture the evolving thermohaline characteristics of each water mass and allowing us to assess their changing contributions to Indian Ocean OMZs more accurately.

**Table 1. Literature values of water mass properties**

| Water masses | References | Pot. Temp. (°C) | Salinity | PDA (kg m$^{-1}$) | Oxygen (µmol kg$^{-1}$) | Phosphate (µmol kg$^{-1}$) | Nitrate (µmol kg$^{-1}$) |
|---|---|---|---|---|---|---|---|
| **PGW** | Acharya and Panigrahi (2016) | 18.11 | 36.5 | - | 43.75 | 2.12 | 21.05 |
| | (Kumar & Prasad, 1999) | 19-13 | 37.9-35.1 | 26.2-26.8 | - | - | - |
| **AS PGW** | Coatanoan et al 1999 | 15 | 35.8 | 26.59 | 9 | 2.4 | 20 |
| **AS RSW** | | 10 | 35.3 | 27.18 | 22.33 | 2.6 | 30 |
| **RSW** | Acharya and Panigrahi (2016) | 12.55 | 36.2 | - | 28 | 2.38 | 30.46 |
| | (Kumar & Prasad, 1999) | 11-9 | 35.6-35.1 | 27.0-27.4 | - | - | - |
| **PGW/RSW** | Hupe and Karstensen (2000) | 18.7 | 37.69 | ~ 27.1 | 50 | 1.56 | 19.7 |
| | You and Tomczak (1993) | 25.9 | 38.08 | 25.7 | 161.9 | 0.372 | - |
| | Rixen and Ittekkot (2005) | 27.41 | 36.33 | - | 146.5 | 0.99 | 8.67 |
| **RSIW** | You (1998) | 11.96 | 35.63 | 27.13 | 23.96 | 2.55 | - |
| **mAABW** | Haine et al. (1998) | 0.8 | 34.72 | 28.14 | 245 | - | - |
| **dIDW** | Acharya and Panigrahi (2016) | 0.92 | 34.72 | | 221.47 | 2.12 | 30.53 |
| **LIDW** | Hupe and Karstensen (2000) | 0.38 | 34.7 | | 216 | 2.2 | 32.1 |
| **ICW** | Coatanoan et al. (1999) | 10.2 | 34.8 | 26.76 | 250 | 0.8 | 8 |
| | Rixen and Ittekkot (2005) | 12.45 | 35.11 | < 25 | 126.3 | 1.46 | 21.21 |
| **ICW upper** | Acharya and Panigrahi (2016) | 18 | 35.47 | | 253.41 | 0.11 | 0.01 |
| **ICW lower** | | 9 | 34.54 | | 274.37 | 1.07 | 14.39 |
| **AAIW** | You (1998) | 7.04 | 34.48 | 27.12 | 233.97 | 1.59 | - |
| | Vianello et al. (2017) | 6 | 34.6 | - | - | - | - |
| | de Brauwere et al. (2007) | 3.8-4.0 | 34.35-34.25 | - | - | - | - |
| **ASHSW** | Kumar and Prasad (1999) | 28-24 | 36.7-35.3 | 22.8-24.5 | - | - | - |
| | Vianello et al. (2017) | 28-24 | 35.45-35.3 | - | 196 | - | - |
| **ITFW** | Vianello et al. (2017) | 17-20 | 35.2 | - | 108.93 | - | - |
| **IIW** | You (1998) | 8.16 | 34.69 | 27.13 | 76.25 | 2.28 | - |
| **STSW** | de Brauwere et al. (2007) | 13.28-12.94 | 35.34-34.71 | - | - | - | - |
| | Sokolov and Rintoul (2002) | 11-16.25 | 35.30-35 | - | - | - | - |
| **BoBW** | Parvathi et al. (2014) | 10-5 | 35.1-35.0 | 26-27 | - | - | - |
| **BoBW** | Sengupta et al. (2013) | 24.23-29.66 | 24.97-34.96 | - | - | - | - |

https://doi.org/10.5194/egusphere-2025-4712
Preprint. Discussion started: 12 November 2025


IIW- Indonesian Intermediate water
AS PGW - Arabian Sea Persian Gulf water
AS RSW – Arabian Sea Red Sea water

**Table 2. Properties of water masses included in this study derived from water mass definition**

| Water masses | Potential Temp. (°C) | Salinity | PDA (kg m$^{-1}$) | Oxygen (µmol kg$^{-1}$) | Phosphate (µmol kg$^{-1}$) | Nitrate (µmol kg$^{-1}$) |
|---|---|---|---|---|---|---|
| **PGW** | 17.30[a] | 36.33[a] | 26.47[a] | 15.64 | 2.19 | 21.51 |
| | 17.88[b] | 36.50[b] | 26.45[b] | | | |
| **RSW** | 13.19[a] | 36.02[a] | 27.15[a] | 23.29 | 2.25 | 29.02 |
| | 13.43[b] | 36.06[b] | 27.13[b] | | | |
| **mAABW** | 1.19[a] | 34.9[a] | 27.79[a] | 209.79 | 2.2 | 31.43 |
| | 1.2[b] | 34.9[b] | 27.79[b] | | | |
| **AAIW** | 6.18[a] | 34.52[a] | 27.15[a] | 208 | 1.87 | 29.67 |
| | 6.02[b] | 34.52[b] | 27.17[b] | | | |
| **ASHSW** | 25.43[a] | 36.5[a] | 24.34[a] | 156.84 | 0.75 | 7.64 |
| | 25.58[b] | 36.43[b] | 24.25[b] | | | |
| **ITFW** | 18.10[a] | 34.55[a] | 24.91[a] | 128 | 1.04 | 14.09 |
| | 18.87[b] | 34.59[b] | 24.75[b] | | | |
| **STSW** | 16.86[a] | 35.57[a] | 25.99[a] | 231.82 | 0.34 | 2.68 |
| | 17.95[b] | 35.6[b] | 25.75[b] | | | |
| **BOBW** | 38..37[a] | 33.32[a] | 17.38[a] | 188.18 | 0.23 | 0.3 |
| | 38.59[b] | 33.10[b] | 17.13[b] | | | |
| **Weights** | 36 | 36 | | 14 | 5 | 5 |

Differences in all temperature and salinity value except those highlighted in red are statistically significant with p-values < 0.05
PDA= Potential density anomaly with respect to a reference pressure of 0 dbar,
a = 1995-2004 WOA data
b = 2015-2022 WOA data

https://doi.org/10.5194/egusphere-2025-4712
Preprint. Discussion started: 12 November 2025


**Table 3. The specific latitude, longitude and depth ranges used for each of the water mass definition.**

| Water masses | Latitude | Longitude | Depth range |
|---|---|---|---|
| **PGW** | 21.8° N–24.5° N | 57° E–62° E | 200–300m |
| **RSW** | 11.5° N–13.5° N | 45.3° E–54.5° E | 400–800 m |
| **mAABW** | 50° S–30° S | 45° E–70° E | 3000–5500 m |
| **AAIW** | 47° S–39° S | 45° E–80° E | 500–1000 m |
| **ASHSW** | 17° N–21° N | 61° E–67° E | 5–100 m |
| **ITFW** | 14° S–8° S | 100° E–125° E | 80–300 m |
| **STSW** | 35° S–25° S | 70° E–90° E | 5–300 m |
| **BOBW** | 12° N–18° N | 85° E–91° E | 0–50 m |

## 3 Results and Discussion

Our analysis using WOA data reveals a notable temperature increase across all surface-originating water masses, with the exception of the Antarctic Intermediate Water (AAIW), when comparing the decadal averages between 1995–2004 and 2015–2022 (see Table 2).

To account for the observed warming across of source water masses, we examined NOAA data and found a significant increase in sea surface temperature (SST) across the Indian Ocean between 1981–2025 (Appendix Fig. 10). This warming exceeds what would be expected from alternating ENSO and IOD events, whose opposing phases between decades largely offset their influence on decadal averages. Moreover, the time periods (1995–2004 and 2015–2022), seem to have experienced quite similar climate anomalies. The increase in temperature of the water masses is therefore mostly attributed to global warming. After all, the tropical Indian Ocean has been reported to experience a rapid basin-wide SST increase of approximately 1° C between 1951 and 2015 due to global warming - substantially higher than the global SST increase of 0.7° C during the same period (Roxy et al., 2020).

https://doi.org/10.5194/egusphere-2025-4712
Preprint. Discussion started: 12 November 2025


This increased temperature introduces challenges to the definition of water masses as temperature/salinity (T/S) properties of the source water masses are evolving, despite having previously been treated as constant. Assuming a constant T/S property when defining water masses could lead to incorrect attribution or overestimation of mixing during eOMP analysis. This is especially true when comparing two distant time periods, since a recently formed warmed water mass parcel might not match "parent" water mass from the past. We addressed this challenge by adopting a time-specific water mass definition in our analysis. Therefore, defining the properties of the water masses twice, once for 1995 and again for recent periods as stated earlier. This approach helps us to account for the impact of global warming on water masses in our analysis.

### 3.1 Water mass composition and temporal changes in the Indian Ocean

The central objective of our study is to examine how water mass dynamics influence OMZ behavior in the Indian Ocean. First, we will consider changes in the composition of water masses, focusing on how contributions from remote sources (water masses with southern Indian Ocean pathway) and local sources (water masses formed in the northern Indian Ocean or adjacent seas) have changed over time in response to global warming.

#### 3.1.1 Spatial distribution and regional differences in 1995

The spatial distribution of water mass composition across the Indian Ocean in 1995 reveals distinct regional patterns that reflect varying influences of remote and local water masses. In the western Indian Ocean transect (15° N–30° S, 150–1200 m), the dominant water masses were mAABW (43 %), STSW (29 %), and PGW (11 %). Contributions from ITFW (10 %) were also notable, whereas RSW (1 %), AAIW (2 %), ASHSW (2 %), and BoBW (2 %) contributed relatively little in the western Indian Ocean transect (Fig. 3g).

In the central equatorial Indian Ocean (15° S, 3° N, 150–1200 m), analysis revealed a slightly similar structure, with dominant influence from mAABW (50 %), STSW (22 %) and ITFW (19 %). Contributions from PGW (6 %) was very minimal as those of other water masses and did not significantly contribute to the central equatorial Indian Ocean (Fig. 3g). In the eastern Indian Ocean transect, mAABW was again the most significant contributor (46 %), followed by STSW (22 %) and ITFW (14 %). PGW (7 %), RSW (2 %), ASHSW (2 %), and BoBW (2 %) were present in smaller proportions, similar to the western transect.

These results suggest that in the mid-1990s, southern-sourced and equatorial water masses such as mAABW, STSW and ITFW were prominent throughout the basin. However, the PGW played a more significant role in the western region than in other regions. Meanwhile, the ITFW seems to influence the central and eastern transects more than the western transect.

#### 3.1.2 Distinct characteristics of the Arabian Sea and Bay of Bengal OMZs in 1995

In the northern part of both the western and eastern transects, both the AS OMZ and BoB OMZ reveal $O_2$ concentrations < 20 µmol kg$^{-1}$. These OMZs also exhibit notable differences in their water mass distribution in 1995.

https://doi.org/10.5194/egusphere-2025-4712
Preprint. Discussion started: 12 November 2025


Unlike in the western transects, the AS OMZ was strongly influenced by PGW (47 %), mAABW (28 %), STSW (10 %) and ITFW (5 %), with lesser contributions from RSW (3 %), AAIW (2 %), ASHSW (3 %), and BoBW (2 %) (Fig. 3a). In contrast, the BoB OMZ was dominated by mAABW (38 %), ITFW (21 %), and STSW (17 %), with a relatively minor contribution from PGW (13 %). Contributions from RSW (5 %), BoBW (2 %), AAIW (2 %), and ASHSW (2 %) were all relatively minor in the BoB OMZ (Fig. 3d).

These contrasts demonstrate the differing roles of local and remote water masses to the ventilation of the OMZs in 1995. While the AS OMZ receives substantial ventilation from marginal seas (notably the Persian Gulf), the BoB OMZ relies more on remote water masses.

### 3.1.3 Temporal shifts in water mass contributions.

Over the comparison period, the data reveal a consistent and region-wide shift from local and equatorial water masses towards remote southern-origin waters. Across the western Indian Ocean transect, contributions from STSW and mAABW increased from 29 to 34 % and 42.7 to 43.4 %, respectively, between 1995 and 2018. RSW also exhibited a modest increase from 0.9 to 1.4 %. In contrast, the proportions of PGW, ITFW, AAIW, ASHSW, and BoBW all declined (Fig. 3c), indicating a net reduction in the influence of local and equatorial sources.

Between 1995 and 2018, PGW declined substantially within the AS OMZ core, from 47 to 40 %, while STSW almost doubled from 10 to 18 %. At the same time, mAABW also increased from 28 to 31 %, and RSW rose slightly from 3 to 4 %. Meanwhile, all other water masses exhibited declines, including AAIW (2 to 1 %), ITFW (5.2 to 4.7 %), ASHSW (3 to 1 %), and BoBW (2 to 1 %) (Fig. 3a). Similar to the western Indian Ocean transect, these shifts reflect a net reduction in the influence of local and equatorial sources and increased penetration of waters formed at higher southern latitudes into the AS OMZ. Since we considered only water masses formed at the ocean surface, these findings provide a slightly different perspective compared to previous studies. Earlier research has identified the Indian Central Water (ICW) as the most prominent water mass in the AS OMZ, in association with the RSW and PGW (Hupe & Karstensen, 2000; Rixen & Ittekkot, 2005; Acharya & Panigrahi, 2016; Schmidt et al., 2020). The ICW originates through convective mixing in the southern Indian Ocean (Sverdrup et al., 1942) and it is also a mixture of STSW and ITFW (Schott & McCreary Jr, 2001). The current water mass composition in the Arabian Sea is consistent with previous studies but enables for a direct assessment of the role of water masses originating from the surface, rather than mixtures, in ventilating the OMZ.

In the eastern Indian Ocean transect, between 1995–2016, a similar trend emerged. During that period, mAABW increased from 46 to 50 % and STSW from 22 to 28 %. However, contributions from PGW (7 to 5 %), RSW (2 to 1 %), AAIW (5 to 2 %) and BoBW (2 to 1 %) all declined, suggesting a diminished influence from both the marginal seas and the northern subtropics (Fig. 3f). Furthermore, within the same time period in the BoB OMZ, STSW increased substantially from 17 to 33 %, while all local and equatorial waters declined significantly, including PGW (13 to 6 %), RSW (5 to 2 %), AAIW (2 to 1 %), ITFW (20 to 19 %), ASHSW (2 to 0 %), and BoBW (2 to 1 %) (Fig 3d). The

https://doi.org/10.5194/egusphere-2025-4712
Preprint. Discussion started: 12 November 2025


mAABW remained the dominant contributor, with only a slight increase in the lower OMZ (500–800 m; 52 to 54 %). This enhanced inflow of mAABW could potentially erode the OMZ from below.

**Table 4. Percentage change in water mass composition in the Indian Ocean OMZs**

| Water Mass | Source Region | Category | AS OMZ Δ% (1995–2018) | BoB OMZ Δ% (1995–2016) | Interpretation |
|---|---|---|---|---|---|
| **STSW** | 25–35° S, Subtropical South Indian Ocean | Remote | ↑ 83.26 % | ↑ 96.59 % | Enhanced shallow cell of the Indian Ocean MOC |
| **mAABW** | Antarctic/Southern Ocean | Remote | ↑ 8.62 % | ↑ 2.27 % in lower OMZ | Enhanced shallow cell of the Indian Ocean MOC |
| **PGW** | Persian Gulf | Local | ↓ 15.04 % | ↓ 53.45 % | Shoaling/stratification of regional seas |
| **ASHSW** | Arabian Sea (AS) | Local | ↓ 62.62 % | ↓ 79.78 % | Increased stratification of local surface waters |
| **ITFW** | Indonesian Archipelago | Equatorial | ↓ 8.24 % | ↓ 7.37 % | Decline of Indonesian Throughflow (ITF) |
| **AAIW** | Subantarctic Front | Remote | ↓ 59.39 % | ↓ 69.87 % | Possible changes in mode water formation or flow re-direction |
| **RSW** | Red Sea | Local | ↑ 19.88 % | ↓ 59.34 % | Enhanced shallow cell in the AS OMZ, reduced inflow into the BoB due to weakening monsoon. |
| **BoBW** | Bay of Bengal (BoB) | Local | ↓ 32.26 % | ↓ 58.33 % | Increased stratification of local surface waters |

Temporal changes in the equatorial Indian Ocean (15°S–3°N) also support these basin-wide trends. In the western equatorial transect, between 1995–2018, increases in STSW (27 to 29 %) and mAABW (48 to 50 %) were observed, while PGW (6 to 5 %) and ITFW (17 to 16 %) declined. Other local water masses also showed declines, though their contributions were minimal (Fig. 3b). Between 1995 and 2019/2024, the central equatorial region showed a different pattern, with STSW (22 to 31 %) increasing, while contributions from mAABW (50 to 48 %) and ITFW (19 to 17 %) decreased (Fig. 3g). In the eastern equatorial region between 1995 and 2016, all local water masses declined. However, STSW (25 to 26 %), mAABW (47 to 52 %), and ITFW (17 to 18 %) increased (See Table 4). The rise in ITFW is likely linked to its proximity to the ITF source region in the eastern basin (Fig. 3e). Collectively, these results point to

https://doi.org/10.5194/egusphere-2025-4712
Preprint. Discussion started: 12 November 2025


a consistent, basin-wide shift in water mass composition, characterized by a decline in the role of local and equatorial water masses (PGW, RSW, ASHSW, BoBW and ITFW) and an increasing impact of remote water masses (mAABW and STSW).

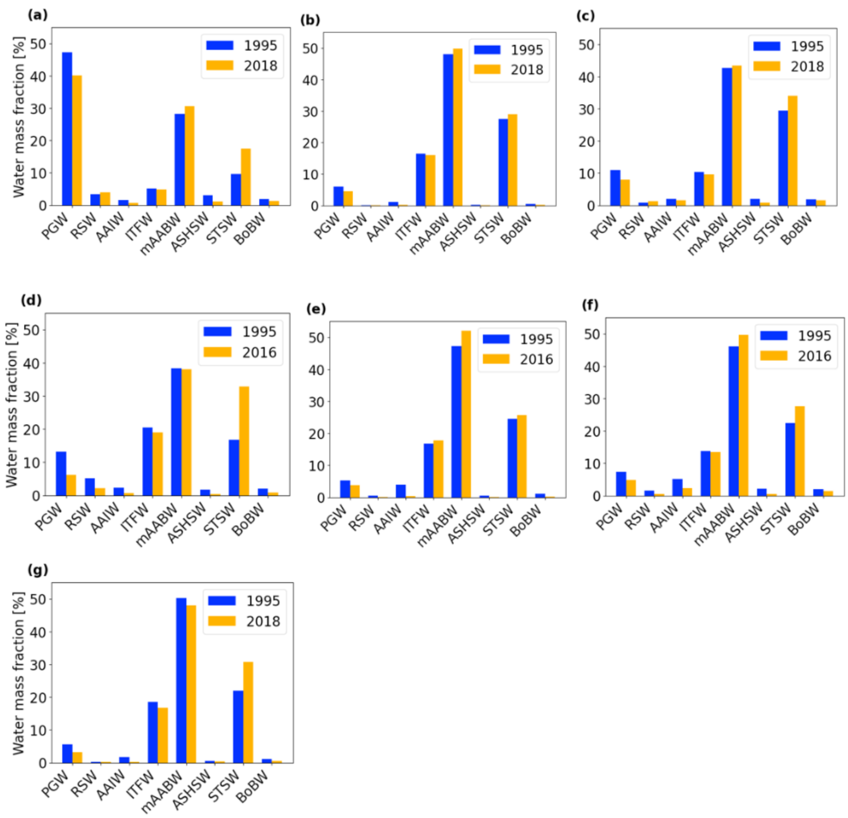


**Figure 3: Water mass fraction in the (a) Arabian Sea OMZ (Dissolved oxygen < 20 µmol kg$^{-1}$) depth 150-1000 m, (b) western equatorial region (15° S – 3° N, depth 150-1200 m) (c) entire western Indian Ocean transect (150-1200 m), (d) Bay of Bengal OMZ (Dissolved oxygen < 20 µmol kg-1 ), depth 150-800 m) (e) eastern equatorial region (15° S – 3° N, depth 150-1200 m) (f) entire eastern Indian Ocean transect (150-1200 m), (g) central equatorial region (15° S – 3° N, depth 150-1200 m).**

### 3.2 Factors contributing to changes in water mass composition

#### 3.2.1 Increased stratification and declining monsoon

All local water masses which dominate the upper 300–450 m including PGW and ASHSW (excluding RSW) experienced a decline in the AS OMZ. Additionally, all local water masses including RSW declined in the BoB OMZ. This decline in local water masses in general may be attributed to increased stratification and reduced vertical mixing

https://doi.org/10.5194/egusphere-2025-4712
Preprint. Discussion started: 12 November 2025


due to increased surface warming in the northern Indian Ocean (Helm et al., 2011; Sridevi et al., 2023). Moreover, a recent study by Roch et al. (2023) reported a global stratification increase of 7 to 8 %, which could have reduced the penetration by local water masses. This trend also aligns with previous studies that have highlighted the impact of ocean warming and increased stratification, which reduce vertical mixing and impede the penetration of marginal water masses into the OMZs (Helm et al., 2011). Furthermore, the decline of RSW, PGW and ASHSW in the BoB OMZ can be attributed to decline in the South Asian summer monsoon (Roxy et al., 2015; Zhou et al., 2008) which can limit the lateral transport of water from the Arabian Sea to the Bay of Bengal through the southwest monsoon current.

### 3.2.2 Implications of the meridional overturning circulation

The increase in mAABW and STSW in the Indian Ocean and its OMZs indicates a reorganization of large-scale ocean circulation such as the global Thermohaline Circulation (THC) and the Indian Ocean MOC under global warming. The decline of the global THC due to global warming has been reported (Caesar et al., 2021; de la Vara et al., 2022; Gou et al., 2024), which has led to the weakening of the ITF inflow in the Indian Ocean and Agulhas leakage into the Atlantic Ocean (Peng et al., 2023; Shen et al., 2023; Großelindemann et al., 2024). The weakening of the ITF could in turn reduce the cross-equatorial flow, thereby allowing increased northward flow of mAABW and STSW into the northern Indian Ocean through transport in the Indian Ocean MOC (see Fig. 4 and 5). Observed shifts in water mass composition across the Indian Ocean, particularly the increased contributions of remote water masses including mAABW and STSW, alongside a decline in local and equatorial water masses including PGW, RSW, ASHSW, BoBW and ITFW, agrees with this concept and indicates a substantial reorganization of the Indian Ocean's MOC. This reorganization reflects a strengthening of both the deep and shallow cells of the Indian Ocean MOC. The strengthening of the deep cell is evidenced by the overall increased contribution of mAABW across the Indian Ocean basin and OMZs, which points to enhanced northward transport of dense bottom waters originating from high southern latitudes. This suggests that the deep cell is now more effective in transporting deep remote water masses reaching even the Arabian Sea. Concurrently, the increased percentage contribution of STSW, especially in the OMZ cores of both the Arabian Sea and the Bay of Bengal, signals a robust intensification of the shallow overturning cell, with stronger inflow from subtropical regions. STSW originates in the southern subtropical Indian Ocean, and its enhanced penetration into the northern basin implies greater surface-to-intermediate water connectivity.

This observed adjustments in circulation patterns also means a southward shift from local to remote water mass sources contributing to the OMZs. Such shift aligns with results by Moffitt et al. (2015), who showed evidence of high degree of coupling between the global climate change and OMZ expansion or shrinkage, suggesting that OMZs dynamically responds to both local and remote water mass input influenced by global warming. Additionally, recent findings by Ditkovsky et al. (2023) also highlights how the southwest Indian Ocean experience increased influx of high-oxygenated waters supplied from the southern Indian Ocean gyre due to a decline in the contribution of the Indonesian Throughflow. This shift would certainly have implications for the physical oxygen supply to the OMZs.

https://doi.org/10.5194/egusphere-2025-4712
Preprint. Discussion started: 12 November 2025


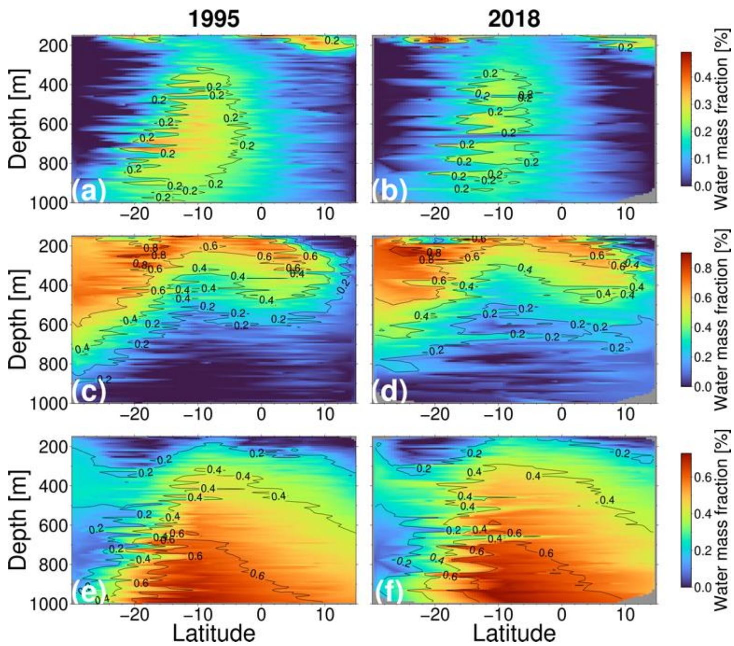


**Figure 4: Temporal changes in water mass fraction in the western Indian Ocean transect for (a) ITFW 1995, (b) ITFW 2018, (c) STSW 1995, (d) STSW 2018, (e) mAABW 1995, (f) mAABW 2018.**

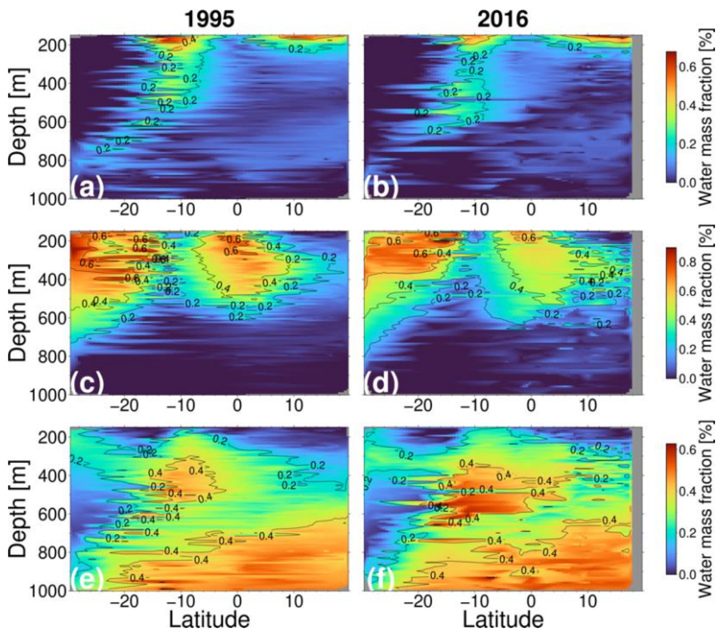

https://doi.org/10.5194/egusphere-2025-4712
Preprint. Discussion started: 12 November 2025


**Figure 5: Temporal changes in water mass fraction in eastern Indian Ocean transect for (a) ITFW 1995, (b) ITFW 2018, (c) STSW 1995, (d) STSW 2018, (e) mAABW 1995, (f) mAABW 2018.**

### 3.3 Physical oxygen supply

Our analysis reveals that the Indian Ocean OMZs have experienced an increase in physical oxygen supply in recent decades due to compositional changes in contributing water masses. Physical oxygen supply patterns identified in this analysis are important for understanding the resilience of the BoB OMZ to global warming as well as the reversal trend of the AS OMZ. Notably, these shifts involve a reduced influence from relatively oxygen-poor local and equatorial water masses (e.g., PGW, RSW, ASHSW, BoBW, and ITFW) and an increased contribution from oxygen-rich remote water masses. Since the physical oxygen supply was calculated in reference to the defined oxygen concentration of the water mass (see. Table 2) and the water mass fraction (see. Eq. 3), their contribution varied substantially within each transect. Overall, the replacement of oxygen-poor water masses by relatively oxygen-rich ones is leading to an increased physical oxygen supply across the Indian Ocean basin as well as the OMZs.

In the western Indian Ocean, AS OMZ, eastern Indian Ocean and BoB OMZ, an increased supply of mAABW and STSW led to an overall increase in average physical oxygen supply. In western Indian Ocean and AS OMZ, physical oxygen supply rose from 184.11 to 191.22 and 107.86 to 123.72 µmol kg$^{-1}$ respectively between 1995 and 2018 (Fig. 6c & 6a). While in the eastern Indian Ocean and BoB OMZ transects, oxygen supply rose from 185.45 to 194.65 and 160.01 to 185.34 µmol kg$^{-1}$ respectively between 1995 and 2016 (Fig. 6c & 6b).
Analysis of equatorial transects also reveals an increase in physical oxygen supply around the equator, primarily due to increase in STSW and mAABW. Overall, the average physical oxygen supply increased from 190.25 to 194.11 µmol kg$^{-1}$ in the western equatorial transect between 1995 and 2018, from 187.56 to 196.04 µmol kg$^{-1}$ in the central equatorial region between 1995 and 2019/2024 and from 189.49 to 193.43 µmol kg$^{-1}$ in the eastern equatorial transect between 1995 and 2016 (Fig. 6c).

Our result show that the decline in oxygen-poor local water masses (e.g., PGW, ASHSW and BoBW) alongside reduced inflow from the ITF, favored the increased influx of oxygen-rich remote water masses from the south leading to increased physical oxygen supply in both OMZs. This aligns with model results suggesting an oxygen increase in the AS OMZ is driven by mixing processes (Oschlies et al., 2017; Ditkovsky et al., 2023; Lachkar et al., 2023; P. Vallivattathillam et al., 2023). The observed increased physical oxygen supply in the OMZs through a shift in water masses can be attributed to changes in the global THC and Indian Ocean MOC due to global warming as discussed earlier. Oxygen-poor local water masses are being replaced by oxygen-rich remote water masses leading to an unexpected trend in physical oxygen supply to the OMZs. Although ongoing global warming is expected to enhance upper-ocean stratification, thereby limiting vertical mixing and oxygen input from local water masses, the influx of oxygen-rich remote water masses is increasing oxygen levels in the OMZs, despite the shoaling of local water masses. For example, high biological productivity and climate-induced low ventilation from PGW have historically been responsible for the expansion of the AS OMZ (Lachkar et al., 2019). Although the input of PGW has decreased, our analysis shows that the increased inflow of more oxygen-rich STSW and mAABW is enhancing the oxygenation in

https://doi.org/10.5194/egusphere-2025-4712
Preprint. Discussion started: 12 November 2025


the OMZ. Furthermore, the Bay of Bengal appears to benefit more from oxygen-rich remote water masses, likely due to efficient mixing such as eddy-driven upwelling (Bhaskar et al., 2021). This may contribute to the less intense BoB OMZ compared to the AS OMZ. Additionally, higher oxygen baseline in the BoB OMZ may amplify the effect of even modest oxygen inflows.

The overall trend suggests that climate-driven circulation changes are restructuring the OMZs. In general, there seems to be a shift in the factors controlling the OMZs from local forcing (e.g., monsoon-driven productivity and local water masses) to remote forcing (southern pathway waters) under a global warming scenario. Historical results obtained from the global atmosphere-ocean model and eddy-resolving regional models, which indicate that the reduced inflow of oxygen-rich waters from the south has contributed to the intensification of the AS OMZ over the past 6,000 years as reported in a review by Rixen et al. (2020). Furthermore, warming-induced deoxygenation in PGW has also been reported to exacerbated the AS OMZ intensity. However, our results indicate a shift, as the OMZ intensity is now been observed to be greatly influenced by remote water masses, suggesting the reversal of a long-term cycle.

Despite these large-scale changes in the physical oxygen supply, the measured increase in dissolved oxygen in the GLODAPv2 data is relatively small, approximately 0.1 µmol kg$^{-1}$ in the AS OMZ and on average 1.69 µmol kg$^{-1}$ in the BoB OMZ (Fig. 6a & 6b). This indicates that biological oxygen consumption rates significantly impacted the overall oxygen level. We therefore need to understand the biological oxygen consumption mechanisms to gain a more complete picture of the OMZs trend.

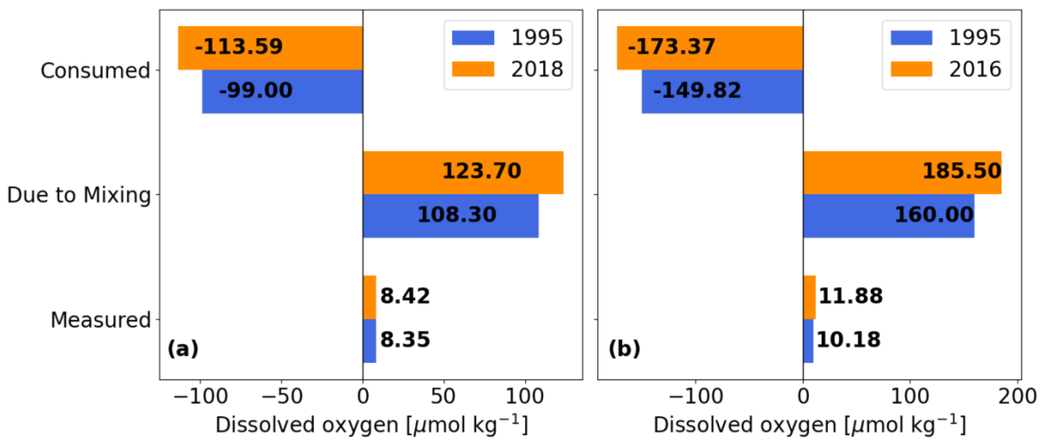

https://doi.org/10.5194/egusphere-2025-4712
Preprint. Discussion started: 12 November 2025


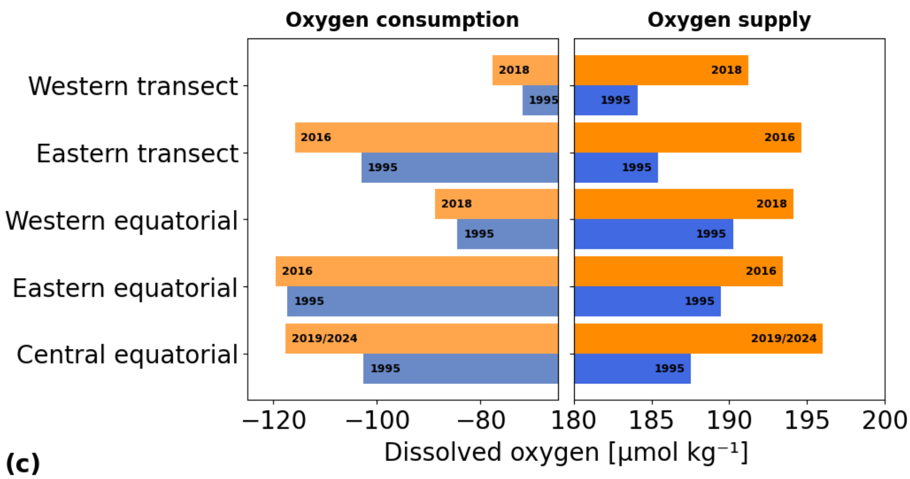


**Figure 6: Average biological oxygen consumption, oxygen supplied due to mixing and oxygen measured in (a) Arabian Sea OMZ, (b) Bay of Bengal OMZ (Dissolved oxygen < 20 µmol kg$^{-1}$ (c) comparing oxygen supply and consumption across the western (1995 and 2018), eastern (1995 and 2016) and equatorial transects (1995 and 2019/2024).**

### 3.4 Biological oxygen consumption

Our study reveals an increase in the physical oxygen supply in the OMZs. However, understanding the balance between oxygen supply and oxygen consumption in the OMZ is critical for assessing the net oxygen concentrations (Rixen et al., 2020). In this section we quantify oxygen consumption to provide a clearer picture of the dissolved oxygen dynamics of the Indian Ocean OMZs.

Analysis of data across the entire transects reveals an increase in biological oxygen consumption. In the western transect, oxygen consumption rose from -71.88 to -77.60 µmol kg$^{-1}$ between 1995 and 2018, while in the eastern transect it rose from -103.00 to -115.85 µmol kg$^{-1}$ between 1995 and 2016 (Fig. 6c). Similarly, the equatorial transects exhibited a comparable upward trend; biological oxygen consumption increased from -84.46 to -88.85 µmol kg$^{-1}$ in the western equatorial transect between 1995 and 2018, from -102.59 to -117.68 µmol kg$^{-1}$ in the central equatorial region between 1995 and 2019/2024, and from -117.28 to -119.53 µmol kg$^{-1}$ in the eastern equatorial transect between 1995 and 2016 (Fig. 6c).

Furthermore, analysis indicates a significant increase in biological oxygen consumption in both AS OMZ and BoB OMZ ($O_2$ < 20 µmol kg$^{-1}$). In the AS OMZ, oxygen consumption increased from an average of -98.72 µmol kg$^{-1}$ in 1995 to -113.94 µmol kg$^{-1}$ in 2018 (Fig. 6a). Similarly, in the BoB OMZ, oxygen consumption rose from approximately -149.82 µmol kg$^{-1}$ in 1995 to -173.21 µmol kg$^{-1}$ in 2016 (Fig. 6b).

https://doi.org/10.5194/egusphere-2025-4712
Preprint. Discussion started: 12 November 2025


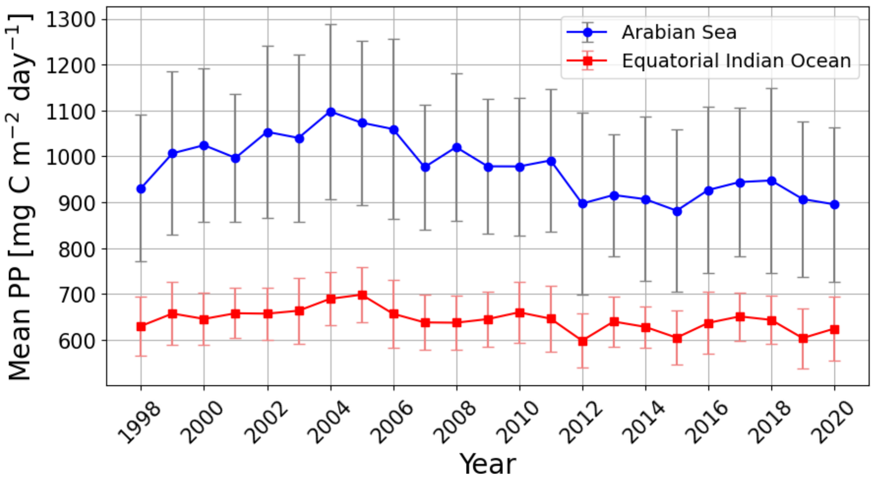


**Figure 7: Mean and standard deviation of annual primary productivity (PP) in the Arabian Sea and Equatorial Indian Ocean.**

Traditionally, the high oxygen consumption in the Indian Ocean OMZs has been attributed to summer monsoon-induced high primary productivity (Rixen et al., 1996; Wiggert et al., 2006). However, recent studies suggest a weakening of the summer monsoon (Zhou et al., 2008; Roxy et al., 2015). Additionally, increasing equatorial oxygen concentrations have been linked to decreasing oxygen consumption (Kwiatkowski et al., 2020), which also aligns with declining primary productivity (PP) in the Arabian Sea/Equatorial Indian Ocean since 2005 observed from analysis of PP data (Fig. 7). Despite this reported trend, our analysis shows an increasing oxygen consumption, suggesting that alternative mechanisms are at play. One possible explanation for this increased biological oxygen consumption is a longer residence time of water masses in the Indian Ocean and it's OMZs, especially in the BoB OMZ. This means water masses are trapped within the OMZs for longer period, prolonging its exposure to remineralization processes (Cavan et al., 2017). This increased residence time may be driven by the slowdown in the global THC, which is closely linked to reduced transport through the Indonesian Throughflow (ITF) and Agulhas Current. These are both key components of the inter-ocean exchange system with the global THC (Broecker, 1991; Durgadoo et al., 2017), and have both been recently reported to be weakening (Großelindemann et al., 2024). This means less water exchange in the Indian Ocean (i.e., less inflow through the ITF and less outflow via the Agulhas leakage) resulting in an increase in residence time. The resulting weaker zonal circulation seems to have favored the meridional circulation which carried water from the southern Indian Ocean northwards. This implies a coupling between the OMZ in the Indian Ocean and climate change via the effect of the latter on the global THC. Paleoceangraphic records also indicate a strong link between climate changes in the North Atlantic Ocean and the OMZ (Schulz et al., 1998; Altabet et al., 1999; Suthhof et al., 2001). But in contrasts to our results a warming was associated with an intensification of the OMZ and cooling with a reduced intensification. However, on this paleo-time scales climate changes are linked to sea level changes (Rosenthal et al., 2003; DiNezio & Tierney, 2013) and decreasing sea level must have lowered the ITF during cooler phases which in turn caused enhanced transport of well-oxygenated waters from the south towards the

https://doi.org/10.5194/egusphere-2025-4712
Preprint. Discussion started: 12 November 2025


north as seen today. However today the reduced influx of the ITF is not caused by a sea level drop but changes in the circulation pattern. These are not yet well understood but imply that the current drivers of change vary from those in the past whereas the mechanisms: enhanced residence time, as well as enhanced Indian Ocean meridional circulation due to reduces zone circulation remains the same.

Despite the increase in biological oxygen consumption, the overall rise in measured oxygen concentration in both OMZs (Fig 4) can be explained by the fact that increase in physical oxygen supply from remote water masses outpaced the increase in biological oxygen demand. This indicates a reduction in the size of both the AS OMZ and the BoB OMZ. These results align with the findings of Liu et al. (2024) based on ARGO floats, which reported shrinkage of the AS OMZ since 2013. Model studies from P. Vallivattathillam et al. (2023), who linked the shrinkage of the AS OMZ to robust oxygenation in the southern Arabian Sea, while Ditkovsky et al. (2023) attributed it to the shift in the water mass composition, favoring the influx of oxygen-rich southern pathway remote waters over oxygen-poor ITFW.

## 4 Summary and conclusion

Our study confirms a trend reversal in the expansion of the AS OMZ and also provides new evidence of the shrinkage of the BoB OMZ. It also advances our understanding of how distinct surface-originated water masses contribute to the ventilation of these OMZs. Contrary to expectations regarding the expansion of these OMZs in the context of global warming, our findings reveal that the increased physical oxygen supply via the inflow of oxygen-rich water masses from the southern Indian Ocean is able to compensate for the increased biological oxygen consumption. This leads to a net increase in dissolved oxygen in both the AS OMZ and BoB OMZ. Therefore, we can conclude that there has been a trend reversal in the AS OMZ and a shrinkage of the BoB OMZ in recent times (Fig. 6). This indicates a restructuring of the OMZs, with a shift in the factors controlling the OMZ intensity from monsoon-driven and local water masses to relatively oxygen-rich remote water masses in the context of global warming scenario. This shift is likely linked to the slowdown of the global THC. In the Indian Ocean a weakening of the THC appears to have two effects: (1) reduced passage of ITF through the Indian Ocean, and (2) reduced outflow through the Agulhas leakage into the Atlantic Ocean. This strengthens the influence of the well-oxygenated southern waters, but also enhances the biological oxygen consumption by extending the residence time of water in the OMZ. On paleo-time scales, cooler phases with lowered sea level weakened the ITF, strengthening meridional circulation and enhancing oxygenation in the Indian Ocean. In contrast, today's ITF weakening arises from circulation changes rather than sea level, though the underlying mechanisms remain similar. The current changes indicate the presence of a longer time-scale cycle in the Indian Ocean OMZs which aligns with paleoceanographic archives, however, this cycle seem to be reversing but under a different mechanism compared to the past. Finally, our findings will help improve the representation of the Indian Ocean OMZs in global models, while also indicating the need for continuous monitoring and high-resolution modelling studies to achieve a comprehensive understanding of long-term circulation and oxygen changes in the OMZs under global warming.

## Data and code availability

The dataset and codes to reproduce our result are available for download here https://doi.org/10.5281/zenodo.17191438

## Authors contributions

Cruise data collection: T.R, B.G, N.L Data curation: E.O. Data preparation and analysis: E.O. Funding acquisition: T.R, B.G. PYOMPA package development and code review: A.S. Writing: E.O. Reviews and editing: T.R, B.G, N.L.

## Competing interests

The authors declare that they have no conflict of interest.

## Acknowledgements

We appreciate the effort and contribution of the entire team who participated in the SONNE SO303 cruise in February 2024. Special thanks to PD. Dr. Tim Rixen for his expertise, supervision and numerous reviews to make this manuscript successful. Additionally, we appreciate Dr. Birgit Gaye and Dr. Niko Lahajnar, for their constructive comments which helped improve the manuscript. Furthermore, many thanks to the German Federal Ministry of Education and Research (BMBF), this work was only possible because of their funding (grant number: 03G0303B). Finally, we appreciate the entire team at Leibniz Centre for Tropical Marine Research (ZMT), Bremen for providing a conducive environment and tools needed for research and learning.

## References

Acharya, S. S., & Panigrahi, M. K. (2016). Eastward shift and maintenance of Arabian Sea oxygen minimum zone: Understanding the paradox. *Deep Sea Research Part I: Oceanographic Research Papers*, *115*, 240-252.

Altabet, M. A., Murray, D. W., & Prell, W. L. (1999). Climatically linked oscillations in Arabian Sea denitrification over the past 1 my: Implications for the marine N cycle. *Paleoceanography*, *14*(6), 732-743.

Anderson, L. A., & Sarmiento, J. L. (1994). Redfield ratios of remineralization determined by nutrient data analysis. *Global Biogeochemical Cycles*, *8*(1), 65-80.

Ashok, K., Guan, Z., & Yamagata, T. (2001). Impact of the Indian Ocean dipole on the relationship between the Indian monsoon rainfall and ENSO. *Geophysical Research Letters*, *28*(23), 4499-4502.

Banse, K., Naqvi, S., Narvekar, P., Postel, J., & Jayakumar, D. (2014). Oxygen minimum zone of the open Arabian Sea: variability of oxygen and nitrite from daily to decadal timescales. *Biogeosciences*, *11*(8), 2237-2261.

https://doi.org/10.5194/egusphere-2025-4712
Preprint. Discussion started: 12 November 2025


Beal, L. M., Chereskin, T. K., Lenn, Y. D., & Elipot, S. (2006). The sources and mixing characteristics of the Agulhas Current. *Journal of Physical Oceanography*, *36*(11), 2060-2074.

Beal, L. M., Ffield, A., & Gordon, A. L. (2000). Spreading of Red Sea overflow waters in the Indian Ocean. *Journal of Geophysical Research: Oceans*, *105*(C4), 8549-8564.

Benson, B. B., & Krause Jr., D. (1980). The concentration and isotopic fractionation of gases dissolved in freshwater in equilibrium with the atmosphere. 1. Oxygen. *Limnology and Oceanography*, *25*(4), 662-671. https://doi.org/https://doi.org/10.4319/lo.1980.25.4.0662

Bhaskar, T., Sarma, V. V. S. S., & Kumar, J. P. (2021). Potential Mechanisms Responsible for Spatial Variability in Intensity and Thickness of Oxygen Minimum Zone in the Bay of Bengal. *Journal of Geophysical Research Biogeosciences*, *126*(6). https://doi.org/10.1029/2021jg006341

Bower, A. S., Hunt, H. D., & Price, J. F. (2000). Character and dynamics of the Red Sea and Persian Gulf outflows. *Journal of Geophysical Research: Oceans*, *105*(C3), 6387-6414.

Breitburg, D. L., Grégoire, M., & Isensee, K. (2018). The ocean is losing its breath: Declining oxygen in the world's ocean and coastal waters.

Broecker, W. S. (1991). The Great Ocean Conveyor. *Oceanography*, *4*(2), 79-89.

Cavan, E. L., Trimmer, M., Shelley, F., & Sanders, R. (2017). Remineralization of particulate organic carbon in an ocean oxygen minimum zone. *Nature Communications*, *8*(1), 14847.

Coatanoan, C., Metzl, N., Fieux, M., & Coste, B. (1999). Seasonal water mass distribution in the Indonesian throughflow entering the Indian Ocean. *Journal of Geophysical Research: Oceans*, *104*(C9), 20801-20826.

de Brauwere, A., Jacquet, S. H., De Ridder, F., Dehairs, F., Pintelon, R., Schoukens, J., & Baeyens, W. (2007). Water mass distributions in the Southern Ocean derived from a parametric analysis of mixing water masses. *Journal of Geophysical Research: Oceans*, *112*(C2).

DiNezio, P. N., & Tierney, J. E. (2013). The effect of sea level on glacial Indo-Pacific climate. *Nature Geoscience*, *6*(6), 485-491.

Ditkovsky, S., Resplandy, L., & Busecke, J. (2023). Unique ocean circulation pathways reshape the Indian Ocean oxygen minimum zone with warming. *Biogeosciences*, *20*(23), 4711-4736.

Durgadoo, J. V., Rühs, S., Biastoch, A., & Böning, C. W. B. (2017). Indian Ocean sources of Agulhas leakage. *Journal of Geophysical Research: Oceans*, n/a-n/a. https://doi.org/10.1002/2016JC012676

Duteil, O., & Oschlies, A. (2011). Sensitivity of Simulated Extent and Future Evolution of Marine Suboxia to Mixing Intensity. *Geophysical Research Letters*, *38*(6), n/a-n/a. https://doi.org/10.1029/2011gl046877

Ekau, W., Auel, H., Pörtner, H. O., & Gilbert, D. (2010). Impacts of hypoxia on the structure and processes in pelagic communities (zooplankton, macro-invertebrates and fish). *Biogeosciences*, *7*(5), 1669-1699. https://doi.org/10.5194/bg-7-1669-2010

Gadgil, S., Rajeevan, M., & Francis, P. A. (2007). Monsoon variability: Links to major oscillations over the equatorial Pacific and Indian oceans. *Current science*, *93*(2), 182-194. http://www.scopus.com/inward/record.url?eid=2-s2.0-34548306755&partnerID=40&md5=60bb11343a5a96da32b5274d530959bc

Gaye, B., Andersch, T., Bartsch, P., Cosmus, H., Dähnke, K., Dasbach, D., Eisnecker, P., Gök, I., Harms, N., Hubert-Huard, R., Hüge, F., John, F., Keuter, S., Kretzschmann, L., Lahajnar, N.,

https://doi.org/10.5194/egusphere-2025-4712
Preprint. Discussion started: 12 November 2025


Lisitano, L., Lüdmann, T., Markfort, G., Meiritz, L.,…Waniek, J. J. (2024). *BIOGeochemistry in the equatorial INdian Ocean - BIOGIN-IIOE2, Cruise No. SO303, 23.01.2024 - 19.02.2024, La Réunion (France) - Colombo (Sri Lanka)* (2510-764X). (SONNE-Berichte, Issue. https://www.tib.eu/de/suchen/id/awi%3A88a51862faa147564c8733c2667e0330f7b0a87a

Goes, J., Tian, H., Gomes, H. d. R., Anderson, O., Al-Hashmi, K., deRada, S., Luo, H., Al-Kharusi, L., Al-Azri, A., & Martinson, D. (2020). Ecosystem state change in the Arabian Sea fuelled by the recent loss of snow over the Himalayan-Tibetan Plateau region, Sci. Rep., 10, 7422. In.

Gordon, A. L., Sprintall, J., Van Aken, H. M., Susanto, D., Wijffels, S., Molcard, R., Ffield, A., Pranowo, W., & Wirasantosa, S. (2010). The Indonesian throughflow during 2004–2006 as observed by the INSTANT program. *Dynamics of Atmospheres and Oceans*, *50*(2), 115-128. https://doi.org/http://dx.doi.org/10.1016/j.dynatmoce.2009.12.002

Gordon, A. L., Susanto, R. D., & Vranes, K. (2003). Cool Indonesian throughflow as a consequence of restricted surface layer flow. *Nature*, *425*, 824-828.

Großelindemann, H., Castruccio, F. S., Danabasoglu, G., & Biastoch, A. (2024). Long-term Variability and Trends of Agulhas Leakage and its Impacts on the Global Overturning. *EGUsphere*.

Haine, T. W., Watson, A. J., Liddicoat, M. I., & Dickson, R. R. (1998). The flow of Antarctic bottom water to the southwest Indian Ocean estimated using CFCs. *Journal of Geophysical Research: Oceans*, *103*(C12), 27637-27653.

Helm, K. P., Bindoff, N. L., & Church, J. A. (2011). Observed decreases in oxygen content of the global ocean. *Geophysical Research Letters*, *38*(23).

Hood, R. R., Beckley, L. E., & Wiggert, J. D. (2017). Biogeochemical and ecological impacts of boundary currents in the Indian Ocean. *Progress in Oceanography*, *156*, 290-325. https://doi.org/https://doi.org/10.1016/j.pocean.2017.04.011

Hupe, A., & Karstensen, J. (2000). Redfield stoichiometry in Arabian Sea subsurface waters. *Global Biogeochemical Cycles*, *14*(1), 357-372.

Johnson, K. S., Riser, S. C., & Ravichandran, M. (2019). Oxygen variability controls denitrification in the Bay of Bengal oxygen minimum zone. *Geophysical Research Letters*, *46*(2), 804-811.

Kämpf, J., & Chapman, P. (2016). Upwelling Systems of the World. In J. Kämpf & P. Chapman (Eds.), *Upwelling Systems of the World*. Springer.

Kulk, G., Platt, T., Dingle, J., Jackson, T., Jönsson, B. F., Bouman, H. A., Babin, M., Brewin, R. J., Doblin, M., & Estrada, M. (2020). Primary production, an index of climate change in the ocean: satellite-based estimates over two decades. *Remote Sensing*, *12*(5), 826.

Kumar, S. P., Madhupratap, M., Kumar, M. D., Gauns, M., Muraleedharan, P., Sarma, V., & De Souza, S. (2000). Physical control of primary productivity on a seasonal scale in central and eastern Arabian Sea. *Journal of Earth System Science*, *109*(4), 433-441.

Kumar, S. P., & Prasad, T. (1999). Formation and spreading of Arabian Sea high-salinity water mass. *Journal of Geophysical Research: Oceans*, *104*(C1), 1455-1464.

Kwiatkowski, L., Torres, O., Bopp, L., Aumont, O., Chamberlain, M., Christian, J. R., Dunne, J. P., Gehlen, M., Ilyina, T., John, J. G., Lenton, A., Li, H., Lovenduski, N. S., Orr, J. C., Palmieri, J., Santana-Falcón, Y., Schwinger, J., Séférian, R., Stock, C. A.,…Ziehn, T. (2020). Twenty-first century ocean warming, acidification, deoxygenation, and upper-ocean nutrient and

https://doi.org/10.5194/egusphere-2025-4712
Preprint. Discussion started: 12 November 2025


primary production decline from CMIP6 model projections. *Biogeosciences*, *17*(13), 3439-3470. https://doi.org/10.5194/bg-17-3439-2020

Lachkar, Z., Levy, M., Hailegeorgis, D., & Vallivattathillam, P. (2023). Differences in recent and future trends in the Arabian Sea oxygen minimum zone: processes and uncertainties. *Frontiers in Marine Science*, *10*, 1122043.

Lachkar, Z., Lévy, M., & Smith, K. S. (2019). Strong Intensification of the Arabian Sea Oxygen Minimum Zone in Response to Arabian Gulf Warming. *Geophysical Research Letters*, *46*(10), 5420-5429. https://doi.org/10.1029/2018GL081631

Lachkar, Z., Lévy, M., & Smith, S. (2018). Intensification and deepening of the Arabian Sea oxygen minimum zone in response to increase in Indian monsoon wind intensity. *Biogeosciences*, *15*(1), 159-186. https://doi.org/10.5194/bg-15-159-2018

Lauvset, S. K., Lange, N., Tanhua, T., Bittig, H. C., Olsen, A., Kozyr, A., Alin, S., Álvarez, M., Azetsu-Scott, K., Barbero, L., Becker, S., Brown, P. J., Carter, B. R., da Cunha, L. C., Feely, R. A., Hoppema, M., Humphreys, M. P., Ishii, M., Jeansson, E.,…Key, R. M. (2022). GLODAPv2.2022: the latest version of the global interior ocean biogeochemical data product. *Earth Syst. Sci. Data*, *14*(12), 5543-5572. https://doi.org/10.5194/essd-14-5543-2022

Liu, T., Qiu, Y., Lin, X., Ni, X., Wang, L., Li, H., & Jing, C. (2024). Dissolved oxygen recovery in the oxygen minimum zone of the Arabian Sea in recent decade as observed by BGC-argo floats. *Geophysical Research Letters*, *51*(12), e2024GL108841.

Malone, T., Azzaro, M., Bode, A., Brown, E., Duce, R., Kamykowski, D., Kang, S., Kedong, Y., Thorndyke, M., & Wang, J. (2015). Primary Production, Cycling of Nutrients, Surface Layer and Plankton. *Centro Oceanográfico de A Coruña*.

Mantyla, A. W., & Reid, J. L. (1995). On the origins of deep and bottom waters of the Indian Ocean. *Journal of Geophysical Research: Oceans*, *100*(C2), 2417-2439.

Menezes, V. V., Macdonald, A. M., & Schatzman, C. (2017). Accelerated freshening of Antarctic Bottom Water over the last decade in the Southern Indian Ocean. *Science Advances*, *3*(1), e1601426. https://doi.org/10.1126/sciadv.1601426

Moffitt, S. E., Moffitt, R., Sauthoff, W., Davis, C. V., Hewett, K. M., & Hill, T. M. (2015). Paleoceanographic Insights on Recent Oxygen Minimum Zone Expansion: Lessons for Modern Oceanography. *Plos One*, *10*(1), e0115246. https://doi.org/10.1371/journal.pone.0115246

Nayak, A. A., Vinayachandran, P., & George, J. V. (2024). Arabian Sea high salinity core supplies oxygen to Bay of Bengal oxygen minimum zone. *arXiv preprint arXiv:2406.10571*.

Olsen, A., Lange, N., Key, R. M., Tanhua, T., Álvarez, M., Becker, S., Bittig, H. C., Carter, B. R., Cotrim da Cunha, L., Feely, R. A., van Heuven, S., Hoppema, M., Ishii, M., Jeansson, E., Jones, S. D., Jutterström, S., Karlsen, M. K., Kozyr, A., Lauvset, S. K.,…Wanninkhof, R. (2019). GLODAPv2.2019 – an update of GLODAPv2. *Earth Syst. Sci. Data*, *11*(3), 1437-1461. https://doi.org/10.5194/essd-11-1437-2019

Oschlies, A., Duteil, O., Getzlaff, J., Koeve, W., Landolfi, A., & Schmidtko, S. (2017). Patterns of deoxygenation: sensitivity to natural and anthropogenic drivers. *Philosophical Transactions of the Royal Society A: Mathematical, Physical and Engineering Sciences*, *375*(2102), 20160325.

https://doi.org/10.5194/egusphere-2025-4712
Preprint. Discussion started: 12 November 2025


Parvathi, V., Thadathil, P., Rajkumar, M., Prasannakumar, S., Muraleedharan, P., Ravichandran, M., Rao, R., & Gopalakrishna, V. (2014). Quality of temperature and salinity data from Argo profiling floats in the Bay of Bengal.

Peng, Q., Xie, S.-P., Huang, R. X., Wang, W., Zu, T., & Wang, D. (2023). Indonesian throughflow slowdown under global warming: Remote AMOC effect versus regional surface forcing. *Journal of Climate*, *36*(5), 1301-1318.

Phillips, H. E., Tandon, A., Furue, R., Hood, R., Ummenhofer, C. C., Benthuysen, J. A., Menezes, V., Hu, S., Webber, B., Sanchez-Franks, A., Cherian, D., Shroyer, E., Feng, M., Wijesekera, H., Chatterjee, A., Yu, L., Hermes, J., Murtugudde, R., Tozuka, T.,…Wiggert, J. (2021). Progress in understanding of Indian Ocean circulation, variability, air–sea exchange, and impacts on biogeochemistry. *Ocean Sci.*, *17*(6), 1677-1751. https://doi.org/10.5194/os-17-1677-2021

Poole, R., & Tomczak, M. (1999). Optimum multiparameter analysis of the water mass structure in the Atlantic Ocean thermocline. *Deep Sea Research Part I: Oceanographic Research Papers*, *46*(11), 1895-1921.

Prell, W. L., & Kutzbach, J. E. (1992). Sensitivity of the Indian monsoon to forcing parameters and implications for its evolution. *Nature*, *360*(6405), 647-652. http://dx.doi.org/10.1038/360647a0

Qadimi, M., Alizadeh, O., & Irannejad, P. (2021). Impacts of the El Niño-Southern Oscillation on the strength and duration of the Indian summer monsoon. *Meteorology and Atmospheric Physics*, *133*, 553-564.

Resplandy, L., Lévy, M., Bopp, L., Echevin, V., Pous, S., Sarma, V., & Kumar, D. (2012). Controlling factors of the oxygen balance in the Arabian Sea's OMZ. *Biogeosciences*, *9*(12), 5095-5109.

Rixen, T., Baum, A., Gaye, B., & Nagel, B. (2014). Seasonal and interannual variations in the nitrogen cycle in the Arabian Sea. *Biogeosciences*, *11*(20), 5733-5747.

Rixen, T., Cowie, G., Gaye, B., Goes, J., do Rosário Gomes, H., Hood, R. R., Lachkar, Z., Schmidt, H., Segschneider, J., & Singh, A. (2020). Reviews and syntheses: Present, past, and future of the oxygen minimum zone in the northern Indian Ocean. *Biogeosciences*, *17*(23), 6051-6080. https://doi.org/10.5194/bg-17-6051-2020

Rixen, T., Haake, B., Ittekkot, V., Guptha, M., Nair, R., & Schlüssel, P. (1996). Coupling between SW monsoon-related surface and deep ocean processes as discerned from continuous particle flux measurements and correlated satellite data. *Journal of Geophysical Research: Oceans*, *101*(C12), 28569-28582.

Rixen, T., & Ittekkot, V. (2005). Nitrogen deficits in the Arabian Sea, implications from a three component mixing analysis. *Deep Sea Research Part II: Topical Studies in Oceanography*, *52*(14-15), 1879-1891.

Rixen, T., Ittekkot, V., Herundi, B., Wetzel, P., Maier-Reimer, E., & Gaye-Haake, B. (2006). ENSO-driven carbon see saw in the Indo-Pacific. *Journal of Geophysical Research Letters*, *33*(L07606), L07606. https://doi.org/10.1029/2005GL024965

Roch, M., Brandt, P., & Schmidtko, S. (2023). Recent large-scale mixed layer and vertical stratification maxima changes [Original Research]. *Frontiers in Marine Science*, *10*. https://doi.org/10.3389/fmars.2023.1277316

Rosenthal, Y., Oppo, D. W., & Linsley, B. K. (2003). The amplitude and phasing of climate change during the last deglaciation in the Sulu Sea, western equatorial Pacific. *Geophysical Research Letters*, *30*(8).

https://doi.org/10.5194/egusphere-2025-4712
Preprint. Discussion started: 12 November 2025


Roxy, M., Gnanaseelan, C., Parekh, A., Chowdary, J. S., Singh, S., Modi, A., Kakatkar, R., Mohapatra, S., Dhara, C., & Shenoi, S. (2020). Indian ocean warming. *Assessment of climate change over the Indian region: a report of the Ministry of Earth Sciences (MoES), Government of India*, 191-206.

Roxy, M. K., Ritika, K., Terray, P., Murtugudde, R., Ashok, K., & Goswami, B. (2015). Drying of Indian subcontinent by rapid Indian Ocean warming and a weakening land-sea thermal gradient. *Nature Communications*, *6*(1), 7423.

Rudnickas, D., Palter, J. B., Hebert, D., & Rossby, T. (2019). Isopycnal Mixing in the North Atlantic Oxygen Minimum Zone Revealed by RAFOS Floats. *Journal of Geophysical Research Oceans*, *124*(9), 6478-6497. https://doi.org/10.1029/2019jc015148

Saenko, O. A., & Weaver, A. J. (2001). Importance of wind-driven sea ice motion for the formation of Antarctic Intermediate Water in a global climate model. *Geophysical Research Letters*, *28*(21), 4147-4150.

Saji, N., Goswami, B. N., Vinayachandran, P., & Yamagata, T. (1999). A dipole mode in the tropical Indian Ocean. *Nature*, *401*(6751), 360-363.

Sarma, V. V. S. S. (2002). An evaluation of physical and biogeochemical processes regulating perennial suboxic conditions in the water column of the Arabian Sea. *Global Biogeochemical Cycles*, *16*(4), 29-21-29-11. https://doi.org/https://doi.org/10.1029/2001GB001461

Sarmiento, J. L., Gruber, N., Brzezinski, M. A., & Dunne, J. P. (2004). High-latitude controls of thermocline nutrients and low latitude biological productivity. *Nature*, *427*(6969), 56-60. http://dx.doi.org/10.1038/nature02127

Schmidt, H., Czeschel, R., & Visbeck, M. (2020). Seasonal Variability of the Arabian Sea Intermediate Circulation and Its Impact on Seasonal Changes of the Upper Oxygen Minimum Zone. *Ocean Science*, *16*(6), 1459-1474. https://doi.org/10.5194/os-16-1459-2020

Schmidt, H., Getzlaff, J., Löptien, U., & Oschlies, A. (2021). Causes of uncertainties in the representation of the Arabian Sea oxygen minimum zone in CMIP5 models. *Ocean Sci.*, *17*(5), 1303-1320. https://doi.org/10.5194/os-17-1303-2021

Schott, F. A., & McCreary Jr, J. P. (2001). The monsoon circulation of the Indian Ocean. *Progress in Oceanography*, *51*(1), 1-123.

Schulz, H., Von Rad, U., Erlenkeuser, H., & von Rad, U. (1998). Correlation between Arabian Sea and Greenland climate oscillations of the past 110,000 years. *Nature*, *393*(6680), 54-57.

Sengupta, S., Parekh, A., Chakraborty, S., Ravi Kumar, K., & Bose, T. (2013). Vertical variation of oxygen isotope in Bay of Bengal and its relationships with water masses. *Journal of Geophysical Research: Oceans*, *118*(12), 6411-6424.

Shen, C., Moore, J. C., Kuswanto, H., & Zhao, L. (2023). The Indonesian Throughflow circulation under solar geoengineering. *Earth System Dynamics*, *14*(6), 1317-1332.

Shrikumar, A., Lawrence, R., & Casciotti, K. L. (2022). PYOMPA technical note. *ESS Open Archive eprints*, *105*, essoar. 10507053.

Sigman, D. M., & Hain, M. P. (2012). The biological productivity of the ocean. *Nature Education Knowledge*, *3*(10), 21.

Sokolov, S., & Rintoul, S. R. (2002). Structure of Southern Ocean fronts at 140 E. *Journal of Marine Systems*, *37*(1-3), 151-184.

https://doi.org/10.5194/egusphere-2025-4712
Preprint. Discussion started: 12 November 2025


Sridevi, B., Sabira, S., & Sarma, V. (2023). Impact of ocean warming on net primary production in the northern Indian Ocean: role of aerosols and freshening of surface ocean. *Environmental Science and Pollution Research*, *30*(18), 53616-53634.

Sridevi, B., & Sarma, V. (2020). A revisit to the regulation of oxygen minimum zone in the Bay of Bengal. *Journal of Earth System Science*, *129*, 1-7.

Stramma, L., Brandt, P., Schott, F., Quadfasel, D., & Fischer, J. (2002). Winter and summer monsoon water mass, heat and freshwater transport changes in the Arabian Sea near 8° N. *Deep Sea Research Part II: Topical Studies in Oceanography*, *49*(7-8), 1173-1195.

Stramma, L., Johnson, G. C., Sprintall, J., & Mohrholz, V. (2008). Expanding oxygen-minimum zones in the tropical oceans. *Science*, *320*(5876), 655-658. https://doi.org/10.1126/science.1153847

Stramma, L., Schmidtko, S., Levin, L. A., & Johnson, G. C. (2010). Ocean oxygen minima expansions and their biological impacts. *Deep Sea Research Part I: Oceanographic Research Papers*, *57*(4), 587-595. https://doi.org/https://doi.org/10.1016/j.dsr.2010.01.005

Suthhof, A., Ittekkot, V., & Gaye-Haake, B. (2001). Millenial-scale oscillation of denitrification intensitiy in the Arabian Sea during the late Quaternary and its potential influence on atmospheric $N_2O$ and global climate. *Global Biogeochemical Cycles*, *15*, 637-650.

Sverdrup, H. U. (1938). On the Explanation of the Oxygen Minima and Maxima in the Oceans1). *ICES Journal of Marine Science*, *13*(2), 163-172. https://doi.org/10.1093/icesjms/13.2.163

Sverdrup, H. U., Johnson, M. W., & Fleming, R. H. (1942). *The Oceans: Their physics, chemistry, and general biology* (Vol. 1087). Prentice-Hall New York.

Talley, L. D. (1996). Antarctic Intermediate Water in the South Atlantic. In *The South Atlantic: present and past circulation* (pp. 219-238). Springer Berlin Heidelberg. https://doi.org/10.1007/978-3-642-80353-6_11

Tchernia, P. (1980). *Descriptive Regional Oceanography*. Pergamon Press. https://books.google.de/books?id=yPFOAAAAMAAJ

Thushara, V., Vinayachandran, P. N. M., Matthews, A. J., Webber, B. G., & Queste, B. Y. (2019). Vertical distribution of chlorophyll in dynamically distinct regions of the southern Bay of Bengal. *Biogeosciences*, *16*(7), 1447-1468.

Tomczak, M. (1999). Some historical, theoretical and applied aspects of quantitative water mass analysis.

Tomczak, M., & Large, D. G. (1989). Optimum multiparameter analysis of mixing in the thermocline of the eastern Indian Ocean. *Journal of Geophysical Research: Oceans*, *94*(C11), 16141-16149.

Vallivattathillam, P., Lachkar, Z., & Lévy, M. (2023). Shrinking of the Arabian Sea oxygen minimum zone with climate change projected with a downscaled model. *Frontiers in Marine Science*, *10*. https://doi.org/ARTN 1123739

10.3389/fmars.2023.1123739

Vallivattathillam, P., Lachkar, Z., & Lévy, M. (2023). Shrinking of the Arabian Sea oxygen minimum zone with climate change projected with a downscaled model [Original Research]. *Frontiers in Marine Science*, *10*. https://www.frontiersin.org/articles/10.3389/fmars.2023.1123739

https://doi.org/10.5194/egusphere-2025-4712
Preprint. Discussion started: 12 November 2025


Vianello, P., Ansorge, I., Rouault, M., & Ostrowski, M. (2017). Transport and transformation of surface water masses across the Mascarene Plateau during the Northeast Monsoon season. *African Journal of Marine Science*, *39*(4), 453-466.

Vinogradova, N., Lee, T., Boutin, J., Drushka, K., Fournier, S., Sabia, R., Stammer, D., Bayler, E., Reul, N., Gordon, A., Melnichenko, O., Li, L., Hackert, E., Martin, M., Kolodziejczyk, N., Hasson, A., Brown, S., Misra, S., & Lindstrom, E. (2019). Satellite Salinity Observing System: Recent Discoveries and the Way Forward [Review]. *Frontiers in Marine Science*, *6*. https://www.frontiersin.org/articles/10.3389/fmars.2019.00243

Wang, C., & Picaut, J. (2004). Understanding ENSO physics—A review. *Earth's Climate: The Ocean–Atmosphere Interaction, Geophys. Monogr*, *147*, 21-48.

Wiggert, J., Murtugudde, R., & Christian, J. (2006). Annual ecosystem variability in the tropical Indian Ocean: Results of a coupled bio-physical ocean general circulation model. *Deep Sea Research Part II: Topical Studies in Oceanography*, *53*(5-7), 644-676.

Wyrtki, K. (1973). Physical Oceanography of the Indian Ocean. In B. Zeitschel (Ed.), *The Biology of the Indian Ocean* (pp. 18-36). Springer Verlag.

Wyrtki, K., Bennett, E. B., & Rochford, D. J. (1971). Oceanographic atlas of the international Indian Ocean expedition. *(No Title)*.

You, Y. (1998). Intermediate water circulation and ventilation of the Indian Ocean derived from water-mass contributions.

Zhou, T., Yu, R., Li, H., & Wang, B. (2008). Ocean forcing to changes in global monsoon precipitation over the recent half-century. *Journal of Climate*, *21*(15), 3833-3852.